

SCP-2/SCP-X GENE ABLATION EXACERBATES HIGH-CHOLESTEROL DIET
INDUCED HEPATIC LIPID ACCUMULATION

A Thesis

by

DEVON KORTNEY KLIPSIC

Submitted to the Office of Graduate and Professional Studies of
Texas A&M University
in partial fulfillment of the requirements for the degree of

MASTER OF SCIENCE

Chair of Committee,	Ann B. Kier
Committee Members,	Friedhelm Schroeder
	Vincent Gresham
Head of Department,	Roger Smith, III

May 2015

Major Subject: Biomedical Sciences

Copyright 2015 Devon Klipsic

ABSTRACT

While a high-cholesterol diet has previously been shown to induce hepatic lipid accumulation in mice, the role of the intracellular cholesterol binding/transport proteins sterol carrier protein-2/sterol carrier protein-x (SCP-2/SCP-x) in this phenotype is unknown. Therefore, the impact of SCP-2/SCP-x gene ablation (double knockout, DKO) on hepatic and serum lipids as well as hepatic expression of proteins in cholesterol homeostasis was examined in mice fed control- and high-cholesterol diets.

Cryopreserved liver, serum, and bile samples from DKO and wild-type, C57BL/6NCr mice which previously underwent a 29 day diet trial on a control- and high-cholesterol diet were utilized along with phenotypic and food consumption data gathered during the study. Liver, serum and biliary lipids were quantified using standard commercially available diagnostic kits. Hepatic mRNA levels of select genes and expression levels of select hepatic proteins involved in lipid metabolism were quantified via qRT-PCR and standard western blotting techniques.

The high-cholesterol diet alone had no impact on food consumption or body weight gain in WT mice, but elicited hepatic accumulation of free and esterified cholesterol. High-cholesterol diet decreased hepatic expression of the SREBP2 target gene product HMGCR in females, but not other target gene proteins (SR-B1, LDL-R, cHMGCS) in either sex. Concomitantly, high-cholesterol also elicited hepatic glyceride accumulation, especially triglyceride, which was associated with increased hepatic SREBP1 protein and SREBP1 lipogenic target gene expression (*Acc1*, *Fas*).

While the DKO did not alter food consumption, a significant decrease in BW gain was appreciated in both high-cholesterol diet and control-fed mice. The DKO also induced hepatic lipid accumulation in control-fed mice, especially of cholesteryl esters and glycerides, which was associated with: i) loss of SCP-2; ii) concomitant upregulation of L-FABP; and/or iii) increased protein levels of SREBP1 and SREBP2. Finally, DKO exacerbated the high-cholesterol diet-induced hepatic cholesterol and glyceride accumulation, but without further altering levels of SREBP2 target genes. Hepatic lipid secretion was impaired due to loss of SCP-2 and reducing Apo B, L-FABP and MTP protein expression. These findings suggested a potential role for SCP-2 in regulating hepatic accumulation of SREBP1 and SREBP2 proteins consistent with the ability of SCP-2 to facilitate intracellular cholesterol trafficking to endoplasmic reticulum from which SREBPs are derived.

DEDICATION

I would like to dedicate this thesis to a fellow resident, Dr. Ashley Peterson, who passed away unexpectedly during the course of our residency program at Texas A&M University. Ashley was a humble, genuine, and inspiring person who always knew how to make me laugh. Without her friendship, support and guidance, I would not have been able to accomplish all I have in these three short years. To paraphrase Helen Keller, having walked in the dark with Ashley will always be better than walking alone now in the light.

ACKNOWLEDGEMENTS

I would like to thank my committee chair, Dr. Kier, and committee members, Drs. Schroeder and Gresham, for their continued support, guidance and encouragement throughout the course of this research and veterinary residency program.

Thanks also to my fellow residents, former and current, and colleagues within the research lab. I would not have been able to complete my project if it wasn't for their continuous education, guidance and support.

I would like to thank my family and friends for their continuous support throughout my veterinary education, career and specialization. It's been a long journey and I thank you for your patience, understanding and encouragement.

Thanks also go to the department and program staff for making my time at the Comparative Medicine Program and Veterinary Pathobiology Department at Texas A&M University a memorable one.

This work was supported in part by the US Public Health Service/National Institutes of Health Grant (GM31651).

NOMENCLATURE

ABCA1	ATP-binding cassette transporter A1
ABCG5	ATP-binding cassette transporter G5
<i>Abcg5</i>	ATP-binding cassette transporter G5 (mRNA)
ABCG8	ATP-binding cassette transporter G8
<i>Abcg8</i>	ATP-binding cassette transporter G8 (mRNA)
ACAT-2	acyl-CoA cholesterol acyltransferase-2
ACBP	acyl-CoA binding protein
<i>Acc1</i>	acetyl CoA carboxylase-1 (mRNA)
<i>Acc2</i>	acetyl CoA carboxylase-2 (mRNA)
Apo A1	apolipoprotein A1
Apo B	apolipoprotein B
ALT	alanine aminotransferase
AST	aspartate aminotransferase
β -HB	beta-hydroxybutyrate
BA	bile acids
BSEP	bile salt export pump
BW	body weight
C	cholesterol
CE	cholesteryl ester
<i>Ceh/Hsl</i>	cholesteryl ester hydrolase, also called hormone sensitive lipase

CPT1A	carnitine palmitoyl transferase-1A
COX4	cytochrome c oxidase subunit 4
CYP7A1	cholesterol 7 α -hydroxylase
CYP27A1	sterol 7 α -hydroxylase
CO	control diet
DKO	SCP-2/SCP-x double null mouse
ER	endoplasmic reticulum
<i>Fas</i>	fatty acid synthetase (mRNA)
FATP-2	fatty acid transport protein-2
FATP-4	fatty acid transport protein-4
FTM	fatty tissue mass
FXR	farnesoid x receptor
GPAT	glycerol-3-phosphate acyltransferase
CH	high cholesterol diet
cHMGCS	cytosolic hydroxymethylglutaryl CoA synthase
<i>Hmgcs</i>	hydroxymethylglutaryl CoA synthase (mRNA)
HMGR	hydroxymethylglutaryl CoA reductase
<i>Hmgcr</i>	hydroxymethylglutaryl CoA reductase (mRNA)
HDL	high density lipoprotein
HDL-C	high density lipoprotein derived cholesterol
LCFA	long chain fatty acid
LCFA CoA	long chain fatty acyl-CoA

LDL	low density lipoprotein
LDL-R	low density lipoprotein receptor
LTM	lean tissue mass
LXR	liver x receptor
L-FABP	liver fatty acid binding protein
miRNA	microRNA
MTP	microsomal triglyceride transfer protein
<i>Mttp</i>	microsomal triglyceride transfer protein coding gene (mRNA)
nonHDL-C	non-high density lipoprotein derived cholesterol
<i>Ntcp</i>	Na ⁺ -taurocholate cotransporting polypeptide (mRNA)
NEFA	non-esterified fatty acid
<i>Oatp1</i>	organic anion transporting polypeptide 1 (mRNA)
<i>Oatp2</i>	organic anion transporting polypeptide 2 (mRNA)
PL	phospholipid
PNS	post-nuclear supernatant
PPAR α	peroxisome proliferator-activated receptor alpha
PCTP	phosphatidylcholine transfer protein
qRT-PCR	quantitative real-time reverse transcriptase polymerase chain reaction
SCP-2	sterol carrier protein 2
SCP-x	sterol carrier protein x, peroxisomal thiolase 2
SDS-PAGE	sodium dodecyl sulfate polyacrylamide gel electrophoresis
SHP	small heterodimer partner

SR-B1	scavenger receptor class B member 1
<i>Srebp1</i>	sterol response element binding protein-1 (mRNA)
SREBP1	sterol response element binding protein-1, (mature 68kDa protein)
Pre-SREBP1	sterol response element binding protein-1, (precursor 125kDa form)
<i>Srebp2</i>	sterol response element binding protein-2 (mRNA)
SREBP2	sterol response element binding protein-2, (mature 68kDa protein)
Pre-SREBP2	sterol response element binding protein-1, (precursor 125kDa form)
TBST buffer	10mM Tris-HCl, pH 8, 100mM NaCl, and 0.05% Tween-20
TP	total protein
TG	triglyceride
WT	wild-type C57BL/6NCr mouse

TABLE OF CONTENTS

	Page
ABSTRACT	ii
DEDICATION	iv
ACKNOWLEDGEMENTS	v
NOMENCLATURE	vi
TABLE OF CONTENTS	x
LIST OF FIGURES	xii
LIST OF TABLES	xiii
INTRODUCTION AND LITERATURE REVIEW	1
MATERIALS AND METHODS	4
Materials	4
Animal Study Background	5
Dietary Cholesterol Study Background	6
<i>In vivo</i> Whole Body Composition	7
Serum, Liver, and Bile Collection	8
Liver Histopathology and Serum Markers for Liver Toxicity	8
Lipid Analysis of Serum, Bile and Liver	9
Hepatic mRNA Levels of Genes in Lipid Metabolism	10
Hepatic Levels of Proteins in Lipid Metabolism	11
Statistical Analysis	13
RESULTS	14
Food Intake, Whole Body Phenotype, and Liver Histology	14
A High-Cholesterol Diet Affected Hepatic Lipid Accumulation More in WT Females	16
Hepatic Lipid Accumulation in DKO Mice	17
Serum Lipids	20
Liver Proteins Involved in Basolateral Uptake and Storage of Cholesterol from Serum Lipoproteins	25

	Page
Proteins Involved in Cytosolic Transport/Targeting of Cholesterol	27
Hepatic Proteins Involved in Secretion of Cholesterol and Other Lipids into Serum	30
Nuclear Receptors Involved in Hepatic <i>De Novo</i> Synthesis of Fatty Acids	31
Nuclear Receptors Involved in Hepatic Lipoprotein Secretion <i>De Novo</i> Synthesis of Cholesterol.....	35
Canalicular Membrane Proteins Involved in Biliary Excretion of Cholesterol ...	36
Hepatic, Serum and Biliary Bile Acid Level.....	38
Expression of Proteins Involved in Hepatic Bile Acid Transport	38
Expression of Enzymes Involved in Hepatic Bile Acid and Cholesterol Synthesis.....	40
Nuclear Receptors Involved in Hepatic Bile Acid Synthesis.....	43
 SUMMARY AND DISCUSSION	 44
DKO Effect on Whole Body Phenotype	45
DKO Elicited Hepatic Accumulation of Cholesterol.....	45
DKO Significantly Potentiated the Induced Hepatic Cholesterol Accumulation Observed in Mice Fed a High Cholesterol Diet	47
DKO Increased Hepatic Accumulation of Glycerides	48
DKO Exacerbated the Induced Hepatic Glyceride Accumulation Observed in Mice Fed a High Cholesterol Diet.....	50
DKO Mouse Construct and Study Design Differences in Comparison to a Previous Study.....	51
 CONCLUSION	 53
 REFERENCES	 54

LIST OF FIGURES

	Page
Figure 1	Effects of SCP-2/SCP-x gene ablation and cholesterol rich diet on hepatic lipid concentrations in mice 18
Figure 2	Effects of SCP-2/SCP-x gene ablation and cholesterol rich diet on fatty acid metabolism 19
Figure 3	Effects of SCP-2/SCP-x gene ablation and cholesterol rich diet on serum cholesterol and triacylglycerol composition..... 23
Figure 4	Effects of SCP-2/SCP-x gene ablation and cholesterol rich diet on serum lipoprotein profiles 24
Figure 5	Analysis of key enzymes and receptors involved in the uptake and conversion of cholesterol by quantitative real time PCR (qRT-PCR) and Western blot..... 26
Figure 6	Analysis of key intracellular and membrane cholesterol transporters and examination of proteins involved in lipoprotein packaging by quantitative real time PCR (qRT-PCR) and Western blot 29
Figure 7	Effect of SCP-2/SCP-x gene ablation and cholesterol rich diet on key regulators of fatty acid biosynthesis 32
Figure 8	Effect of SCP-2/SCP-x gene ablation and cholesterol rich diet on key regulators of cholesterol biosynthesis 34
Figure 9	Bile acid levels and hepatic expression of key proteins in bile acid reuptake and biliary excretion 37
Figure 10	Effect of SCP-2/SCP-x gene ablation and cholesterol rich diet on proteins and transcription factors involved in cholesterol synthesis and oxidation to bile acids 42

LIST OF TABLES

	Page
Table 1	Effect of SCP-2/SCP-x gene ablation on total food consumption and body weight gain of mice fed a high-cholesterol diet 15
Table 2	Effect of SCP-2/SCP-x gene ablation, high cholesterol diet and both together on liver parameters 16
Table 3	Effect of SCP-2/SCP-x gene ablation, high cholesterol diet and both together on serum lipids 22

INTRODUCTION AND LITERATURE REVIEW

A major gap in our understanding of intracellular cholesterol transport is the role of hepatic factors that target cholesterol to cholesterol-sensor molecules in the endoplasmic reticulum (ER), which regulate release of SREBPs, nuclear regulatory proteins controlling transcription of a host of genes for receptors and enzymes in cholesterol and fatty acid metabolism (36; 88; 90; 106; 116). Likewise, little is known about hepatic intracellular factors that mediate rapid intracellular transport of high-density lipoprotein (HDL) cholesterol to other intracellular organelles for oxidation to bile acids (peroxisomes) and biliary elimination of cholesterol across the bile canaliculus (20; 78; 91).

Studies *in vitro* and with cultured cells show that the 13 kDa sterol carrier protein-2 (SCP-2) is a cholesterol binding protein (17; 43; 61; 76; 93; 95; 109; 124) that markedly enhances cholesterol transfer from isolated plasma membranes as well as from lysosomes or lysosomal membranes to plasma membranes, ER, and mitochondria (3; 23; 24; 26; 27; 30; 31; 41; 65; 92; 111; 123). SCP-2 overexpression increases cholesterol uptake, cholesterol transfer from plasma membranes to ER for esterification, and cholesteryl ester accumulation in L-cell fibroblasts (11; 74; 108). SCP-2 is an intracellular binding partner with caveolin-1 and SR-B1, and preferentially enhances cholesterol trafficking from cholesterol-rich plasma membrane microdomains in which these receptors are abundantly distributed (3; 8; 98; 110; 111; 127). These findings suggest a role for SCP-2 in rapid cholesterol intracellular trafficking of LDL-derived

cholesterol to ER for esterification or regulating SREBP release. It is important to note that SCP-2 and SCP-x proteins also contribute to rapid clearance of HDL-cholesterol by facilitating biliary bile acid synthesis (110; 112). By binding and transferring cholesterol to ER, SCP-2 stimulates hepatic cholesterol 7 α -hydroxylase, the rate-limiting enzyme in hepatic bile acid synthesis (51; 105). Through an alternate transcription site, the SCP-2/SCP-x gene also encodes a larger protein, sterol carrier protein-x (SCP-x) (29; 103). SCP-x is the only known enzyme catalyzing the peroxisomal oxidation of cholesterol's branched side chain to form bile acids (29; 103). Canalicular secretion of bile acid drives biliary cholesterol secretion (84; 89; 115).

In vivo support for roles of the SCP-2/SCP-x gene in hepatic cholesterol metabolism and biliary cholesterol secretion comes from studies in both humans and mice. A human SCP-2/SCP-x genetic variation inhibits cholesterol metabolism (19). It must be noted, however, that the human studies were performed with only a single patient (19). In mice, SCP-2 overexpression (2; 5; 125), SCP-2 antisense treatment (83), and SCP-2/SCP-x gene ablation (25; 50; 104) significantly impact hepatic cholesterol metabolism and biliary excretion. However despite the fact that hepatic SCP-x expression is several fold lower in female mice and humans (6; 9), almost all rodent studies have been conducted with male mice (2; 5; 25; 50; 83; 104; 125). Studies regarding the impact of SCP-2 on response to high cholesterol diet are even more limited. Only a single study has examined the effect of SCP-2 overexpression on high-cholesterol fed mice and that only in males (5). The impact of SCP-2/SCP-x gene ablation (DKO) in the context of a high-cholesterol diet is unknown in either sex. Thus

the current study examined the impact of DKO on hepatic cholesterol and biliary phenotype of male and female mice fed a high-cholesterol versus control diet.

MATERIALS AND METHODS

Materials

Rabbit polyclonal antibodies were purchased from the following sources: anti-peroxisome proliferator-activated receptor-alpha (PPAR α ; PA1-822A) from ThermoFisher Scientific (Rockford, IL); anti-ATP-binding cassette transporter (ABCA1; NB400-105) and anti-scavenger receptor class B type 1 (SR-B1; NB400-104) from Novus Biologicals (Littleton, CO); anti-HMG-CoA synthase (cHMGCS; sc-33829), anti-small heterodimer protein (SHP; sc-30169), anti-sterol regulatory element-binding protein 1 (SREBP1; recognizing both 68kDa and 125kDa, sc-367), and anti-sterol regulatory binding protein-2 (SREBP2; recognizing both mature 68kDa and endoplasmic reticulum precursor 125kDa pre-SREBP2, sc-8151) from Santa Cruz Biotechnology (Santa Cruz, CA). Anti-sterol carrier protein 2 (recognizing 58 kDa SCP-x, 15 kDa pro-SCP-2, and 13.2 kDa SCP-2, as previously described) (10); and anti-acyl cholesterol acyltransferase 2 (ACAT2; ab66259), anti-apolipoprotein B (Apo B; ab31992), and anti-cytochrome c oxidase subunit 4 (COX4; ab16056) from Abcam (Cambridge, MA). Goat polyclonal antibodies were obtained from Santa Cruz Biotechnology (Santa Cruz, CA): anti-HMG-CoA reductase (HMGCR; sc-27578), anti-cholesterol-7-alpha-hydroxylase (CYP7A1; sc-14426), anti-sterol-27-hydroxylase (CYP27A1; sc-14835), anti-fatty acid transport protein 2 (FATP-2; sc-161311), anti-fatty acid transport protein 4 (FATP-4; sc-5834), anti-acyl-CoA-binding protein (ACBP; sc-23474), anti-apolipoprotein AI (Apo A1; sc-23606), anti-carnitine palmitoyltransferase I (CPT1; sc-31128); anti-

phosphatidylcholine transfer protein (PCTP; sc-23672); anti-microsomal triglyceride transfer protein (MTP; sc-33116); anti-liver-type fatty acid binding protein (L-FABP; sc-16064); anti-liver X receptor (LXR; sc-1201); anti-farnesoid X receptor (FXR; sc-1205) and anti-low density lipoprotein receptor (LDL-R; sc-11826). All reagents and solvents used for each test method were highest grade available.

Animal Study Background

All animal tissues, serum, and bile samples, along with food consumption and phenotype data, utilized and analyzed for the purpose of this thesis work was procured from a previously performed dietary animal study completed by other lab staff.

The experimental protocol for the use of the research animals was approved by the Institutional Animal Care and Use Committee at Texas A&M University. Male and female inbred C57BL/6NCr mice were acquired from the National Cancer Institute (Frederick Cancer Research and Development Center, Frederick, MD). SCP-2/SCP-x null (DKO) mice on the same C57BL/6NCr background were generated and backcrossed to C57BL/6NCr to the N6 generation as described (8). Mice were fed a standard rodent chow mix [5% calories from fat; D8604 Teklad Rodent Diet, Teklad Diets (Madison, WI)] and were maintained in barrier cages on ventilated racks under a 12:12 light-dark cycle in a temperature controlled facility (25⁰C) with access to food and water ad libitum until study initiation. All animals were sentinel monitored quarterly and confirmed free of all known rodent pathogens.

Dietary Cholesterol Study Background

Seven-week-old male and female wild-type (WT) and SCP-2/SCP-x null (DKO) mice on the C57BL/6NCr background were transferred to a control modified AIN-76A phytoestrogen-free, phytol-free control diet (5% calories from fat; D11243, Research Diets, New Brunswick, NJ) one week prior to beginning the 29 day dietary study. The phytoestrogen-free, phytol-free diet was chosen to minimize any potential complicating effect in sex comparisons due to phytoestrogens, which exert estrogenic effects in mice (113; 114) and from phytol metabolites (e.g. phytanic acid), potent ligand inducers of PPAR α (18; 33; 122). After one week, a total of 56 male and female mice were randomized into 8 groups, with half remaining on the control (CO) modified AIN-76A diet while the other half were placed on a high cholesterol (CH) diet (D01091702, Research Diets, New Brunswick, NJ) composed of the modified AIN-76A control diet supplemented with 1.25% cholesterol and isocaloric to the control diet. Seven mice were assigned to each group: male WT on CO, male DKO on CO, male WT on CH, male DKO on CH, female WT on CO, female DKO on CO, female WT on CH, and female DKO on CH.

Animals were provided with ad libitum food and water throughout the study and maintained singly housed so that individual food intake and body weight could be monitored every other day. Body weights and food intake were measured at approximately the same time of day at each recording. To measure food intake, the bedding was strained for any remaining pellets within the cage as well as any food in the receptacle and the total food remaining was weighed. To more clearly visualize any

small feed particles in the cage and improve food consumption accuracy, diets were color-coded (yellow, CO; blue, CH). Food consumption and body weight data generated from this study was analyzed for statistical significance between the previously defined eight groups.

In vivo Whole Body Composition

Previously performed by other lab staff, mouse total body lean tissue mass (LTM) and fat tissue mass (FTM) was determined *in vivo* by dual-energy X-ray absorptiometry (DEXA) using a Lunar PIXImus densitometer (Lunar Corp., Madison, WI) as previously described (9). The DEXA instrument was calibrated using a phantom mouse with known bone mineral density and fat tissue mass as described (9; 77). DEXA was performed on individual mice at the beginning of the dietary study after mice were fasted overnight (approximately 12 hours) and anesthetized [100 mg/kg ketamine and 10 mg/kg xylazine, administered intraperitoneal (IP) as described (9)]. At the end of the study (day 30), DEXA was similarly performed except the mice were euthanized prior to DEXA. DEXA allowed resolution of bone mass and tissue mass for further resolution into LTM and FTM as described (9; 77).

Previously performed DEXA data was analyzed for statistically significant alterations in LTM and FTM between the previously defined groups.

Serum, Liver, and Bile Collection

The serum, liver and bile previously procured by other lab staff in the following described methods, were utilized for the work covered within this thesis.

On day 29 of the study, mice were fasted overnight (~12 hours) to decrease the influence of recent digestion on serum and liver lipid levels. On day 30, after anesthesia, blood was collected via cardiac puncture, followed by humane euthanasia by cervical dislocation. Blood was stored overnight at 4°C, centrifuged at maximum speed for 20 minutes and serum collected and stored at -80°C. Gall bladders containing bile and livers were separately harvested, and livers weighed and sectioned. Part of the liver was transferred to a RNA stabilization buffer, RNAlater (Ambion, Austin, TX) and stored at -20°C. All remaining tissue samples collected were flash frozen on dry ice and stored at -80°C for future analysis.

Liver Histopathology and Serum Markers of Liver Toxicity

Liver slices near the porta hepatis were fixed for 24 h in 10% neutral buffered formalin, placed in individual cassettes, stored in 70% alcohol, and processed and embedded in paraffin as described (9; 56). Sections cut 4-6 microns in thickness were hematoxylin and eosin stained for histological evaluation (9; 56). Histologic preparation of the above described liver sections and histopathological interpretation was performed previously by other lab staff.

Levels of serum aspartate aminotransferase (AST), alanine aminotransferase (ALT) and beta-Hydroxybutyrate (β -HB) were quantified utilizing Stanbio diagnostic

kits (Boerne, TX). These levels were compared to normal reference ranges to evaluate whether liver toxicity was indicated and then further analyzed for statistical significance between defined groups.

Lipid Analysis of Serum, Bile and Liver

Approximately 0.1g (wet weight) portions of liver from each mouse were homogenized in 0.5mL phosphate buffered saline (pH 7.4) using a motor-driven pestle (Tekmar Co, Cincinnati, OH) operated at 2000 rpm for 5 minutes. Protein concentrations of liver homogenate samples were determined by Bradford protein micro-assay from Bio-Rad Laboratories (Cat # 500-0001, Hercules, CA) as per manufacturer protocol. Costar 96-well assay plates (Corning, Corning, NY) and a Bio Tek Synergy 2 micro-plate reader (Bio Tek Instruments, Winooski, VT) were utilized for the liver lipid, serum and bile assays. Liver homogenate and serum lipids were quantified utilizing Wako diagnostic kits (Richmond, VA) to determine: total cholesterol (TC), free cholesterol (FC), triglyceride (TG), phospholipid (PL) and HDL cholesterol (HDL-C). Liver and serum cholesterol ester (CE) concentrations were calculated by subtracting liver and serum FC from TC. Serum nonHDL-C concentration was calculated by subtracting serum HDL-C from TC. Serum apolipoprotein A1 (Apo A1), serum apolipoprotein B (Apo B) and serum, liver and bile total bile acids (BA) were quantified using the Diazyme diagnostic kit (Ponwy, CA). Biliary cholesterol levels were quantified utilizing Wako diagnostic kit (Richmond, VA). All commercially available diagnostic kits were

utilized according to the manufacturer's instructions, modified for use with 96-well plates and micro-plate reader as described above.

Hepatic mRNA Levels of Genes in Lipid Metabolism

Total RNA was isolated from liver and purified using the RNeasy mini kit (Qiagen, Valencia, CA) using the manufacturer's standard protocol. Nucleic acid concentration and quality were determined by a NanoDrop 1000 Spectrophotometer (Thermo Scientific, Waltham, MA). Samples were stored at -80°C. qRT-PCR expression patterns were analyzed with an ABI PRISM 7000 sequence detection system (Applied Biosystems®, Foster City, CA) using TaqMan® RNA-to-CT™ 1-Step PCR Master Mix Reagent kit, gene-specific TaqMan PCR probes and primers, and the following thermal cycler protocol: 48°C for 30 min, 95°C for 10min, 95°C for 0.15 min and 60°C for 1.0 min, repeated a total of 60 cycles. TaqMan® gene expression assays for specific probes and primers were obtained from Life Technologies™ (Carlsbad, CA) to determine hepatic mRNA levels of: organic anion transporting polypeptide 1 (*Oatp1/Slco1a1*; Mm01267414_m1), organic anion transporting polypeptide 2 (*Oatp2/Slco1c1*; Mm00460672_m1), ATP-binding cassette sub-family G member 5 (*Abcg5*; Mm01226965), ATP-binding cassette sub-family G member 8 (*Abcg8*; Mm00445977_m1), Cholesteryl ester hydrolase/hormone sensitive lipase (*Ceh/Hsl*; Mm00495359_m1), Na⁺-taurocholate co-transporting polypeptide (*Ntcp/Slc10a1*; Mm01302718), Bile salt export pump (*Bsep/Abcb11*; Mm00445168_m1), acetyl CoA carboxylase-1 (*Acc1*; Mm01304285_m1); acetyl CoA carboxylase-2 (*Acc2*;

Mm01204657_m1); fatty acid synthase (*Fas*; Mm00662319_m1), sterol regulatory element binding protein-1 (*Srebp1*; Mm00550338_m1), and sterol regulatory element binding protein-2 (*Srebp2*; Mm01306289_m1). Two replicates of each sample reaction (20µL total volume each) were performed on 96 well optical reaction plates (Applied Biosystems®, Foster City, CA). ABI Prism 7000 SDS software (Applied Biosystems®, Foster City, CA) established the threshold cycle from each well. qRT-PCR data were normalized to the housekeeping gene 18S RNA for mRNA expression of *Oatp1*, *Oapt2*, *Abcg5*, *Abcg8*, *Ceh/Hsl*, *Ntcp*, *Bsep*, *Acc1*, *Acc2*, *Fas*, *Srebp1*, and *Srebp2* made relative to the control mouse group (male WT mice on control diet) for final calculations.

Hepatic Levels of Proteins in Lipid Metabolism

Western blot analysis was performed to determine expression levels of select proteins in liver. Liver samples were homogenized and centrifuged at 4°C at 1,000xg for 5 min to isolate the post nuclear supernatant (PNS). Protein concentrations of the individual PNS samples were established using a Bradford protein assay (Bio-Rad, Hercules, CA). Western blot analyses were performed to determine relative protein levels of: acyl CoA binding protein (ACBP), acyl CoA cholesteryl acyl transferase-2 (ACAT2), ATP-binding cassette sub-family A member 1 (ABCA1), apolipoprotein A1 (Apo A1), apolipoprotein B (Apo B), Cytochrome c oxidase subunit 4 (COX-4), carnitine palmitoyl acyltransferase A1 (CPT1), cytochrome P7A1 (CYP7A1), cytochrome P27A1 (CYP27A1), cytosolic hydroxymethylglutaryl CoA synthase (cHMGCS), fatty acid transport protein 2 (FATP-2), fatty acid transport protein 4

(FATP-4), hydroxymethylglutaryl CoA reductase (HMGCR), liver fatty acid binding protein (L-FABP), low density lipoprotein receptor (LDLR), peroxisome proliferator activated receptor α (PPAR α), phosphatidylcholine transfer protein (PCTP), scavenger receptor B1 (SR-B1), small heterodimer partner (SHP), sterol carrier protein-2 (SCP-2), sterol carrier protein-x (SCP-x), sterol regulatory element binding protein (SREBP1, 68 kDa and 125 kDa forms), sterol regulatory element binding protein (SREBP2, 68 kDa and 125 kDa forms), farnesoid x receptor (FXR), liver x receptor (LXR) and microsomal triglyceride transport protein (MTP).

PNS (10-30 μ g protein) proteins were resolved by Sodium dodecyl sulfate – polyacrylamide gel electrophoresis (SDS-PAGE) using a dual slab gel system (DSG-200, C.B.S. Scientific Inc., San Diego, CA) at 150 volts until visible separation of the molecular weight marker as described (8). The separated proteins were then transferred to a nitrocellulose membrane (Bio-Rad, Cat#162 0112) by electroblotting using the electroblotting system EBU-102 (C.B.S. Scientific Inc., San Diego, CA) in a western transfer buffer (200mM glycine, 12.5mM Tris base in 20% methanol v/v) at 500 mAmps, on ice, for 2-3 hours depending on the size of the protein as previously described by our lab (8). Blots were then blocked in 3% gelatin in TBST (10mM Tris-HCl, pH8, 100mM NaCl, and 0.05% Tween-20) from 30 minutes to overnight at room temperature and then incubated for a period of 30 minutes to overnight at room temperature with the appropriate primary antibodies in 1% gelatin in TBST. Following washing three times for 5 minutes with TBST, blots were incubated for a period of 30 to 120 minutes at room temperature within the appropriate secondary antibodies. A final

wash 3 x 5 min. with TBST was completed, followed by a single 5 minute wash in AP buffer (100mM Tris-HCl, pH 9.0, 100mM NaCl, and 10mM MgCl₂) and then exposure to 5-bromo-4-chloro-3-indolyl phosphate nitro blue tetrazolium (Sigma Aldrich, Cat# B6404) until sufficient color development. Development was stopped by washing the blots in double distilled water. Images of the blots were captured using an Epson Perfection V700 Photo scanner (Long Beach, CA). Proteins were quantified by densitometric analysis using ImageJ software (NIH, Bethesda, MD) as described earlier (8).

Statistical Analysis

All result values were stated as the mean +/- standard error of measure (SEM). Statistical analysis was performed using one-way analysis of variance (ANOVA), followed with the Newman-Keuls multiple comparisons test using either GraphPad software (La Jolla, CA) or Sigma Plot software (Systat, San Jose, CA). Statistical significance was assigned to values with $p < 0.05$.

RESULTS

Food Intake, Whole Body Phenotype, and Liver Histology

Neither SCP-2/SCP-x gene ablation (DKO), high-cholesterol diet, nor both together significantly altered total food consumption of male mice (Table 1).

Nevertheless, SCP-2/SCP-x gene ablation alone significantly decreased body weight gain in female but not control fed WT males (Table 1). High-cholesterol diet alone did not significantly alter body weight gain in either WT males or females (Table 1).

Further, feeding a high-cholesterol diet did not prevent the DKO induced reduction in body weight gain or body weight gain/food consumption seen in the DKO females on the control diet (Table 1). DEXA analysis determined that the decreased weight gain observed in the DKO females was largely associated with a decreasing proportion of lean tissue mass (LTM), while the cholesterol diet alone did not significantly alter proportions of FTM or LTM in either WT males or females (Table 1).

Gross and histopathological analysis of liver did not detect any significant alterations due to DKO, high-cholesterol diet, or both combined. Neither cholesterol diet, DKO, nor both significantly altered liver weight, liver weight/body weight, or liver total protein (Table 2). Upon histopathologic analysis, hepatocyte fatty vacuolation was observed within the female and male DKO and WT mice fed high-cholesterol diet and female DKO mice on control diet. Greater lipid droplet accumulation was observed in the females compared to males. No significant hepatocyte necrosis or inflammation was

noted in any of the groups. The reviewing pathologist determined that the liver histological parameters showed no significant lesions in all groups.

Consistent with the lack of significant gross or histopathological liver lesions, serum AST and ALT values in all groups were less than 35 and 60 units/l, respectively, well within the normal range of mouse values for AST and ALT (Blood chemistry and hematology in 8 inbred strains of mice. MPD: Eumorphia1. Mouse Phenome Database web site, The Jackson Laboratory, Bar Harbor, Maine USA. <http://phenome.jax.org> [Cited 29 Oct, 2014]). Thus, liver toxicity did not account for the altered whole body phenotype or serum and hepatic changes observed in response to the DKO and high-cholesterol diet.

	MALE				FEMALE			
	WT		DKO		WT		DKO	
	CO	CH	CO	CH	CO	CH	CO	CH
Total Food consumption (g)	86±3	91±2	91±4	90±4	86±2	88±2	86±1	87±1
Body Weight gain (g)	2.5±0.5	2.7±0.4	2.4±0.6	1.6±0.4	1.9±0.3	2.3±0.2	0.6±0.2*	1.0±0.4*
Body Weight gain per Food Consumption (mg/g)	30±5	30±3	26±5	18±4	22±3	26±3	7±2*	11±4*
LTM change (g)	1.4±0.4	1.3±0.5	0.4±1.2	0.1±0.8	0.2±0.3	0.7±0.4	-0.7±0.4	-0.9±0.3*
FTM change (g)	0.1±0.2	0.5±0.5	1.6±0.5	1.4±0.4	-0.2±0.2	0.1±0.2	0.2±0.2	0.3±0.3

Table 1: Effect of SCP-2/SCP-x gene ablation on total food consumption and body weight gain of mice fed a high cholesterol diet. CO, control; CH, cholesterol; LTM, lean tissue mass; FTM, fat tissue mass. Values represent the mean ± SEM, n=5-7. *Genotype Effect ($P < 0.05$ for DKO vs. WT within the same diet); # Diet Effect [$P < 0.05$ for Control (CO) vs. High cholesterol (CH) diet within the same genotype].

	MALE				FEMALE			
	WT		DKO		WT		DKO	
	CO	CH	CO	CH	CO	CH	CO	CH
Liver Weight (g)	0.9±0.1	1.1±0.1	1.1±0.1	1.0± 0.1	0.8±0.1	0.9±0.1	0.9±0.1	1.0±0.1
Liver Weight per Body Weight (mg/g)	38±2	43±1	40±1	40±1	40±1	50±2	40±2	50±2
Protein (mg/g)	135±10	126±12	122±7	130±11	126±10	141±10	121±10	107±7
Serum ALT (Units/L)	54±4	45±4	41±5	40±5	57±5	48±7	44±5	59±6
Serum AST (Units/L)	30±2	33±4	19±2	22±3	24±1	20±2	20±2	23±2

Table 2: Effect of SCP-2/SCP-x gene ablation, high cholesterol diet and both together on liver parameters. CO, control; CH, cholesterol; ALT, alanine aminotransferase; AST, aspartate aminotransferase. Values represent the mean ± SEM, n=6-7. No significant differences were noted between groups.

A High Cholesterol Diet Affected Hepatic Lipid Accumulation More in WT Females

The high-cholesterol diet alone increased hepatic accumulation of neutral lipids most markedly in WT females, without altering phospholipid levels (Fig 1B, C), while also increasing both neutral and phospholipid in WT males (Fig 1B, C). Within the neutral lipids, the cholesterol diet alone increased total cholesterol (free and esterified) and triglycerides in both the male and female WT groups (Fig 1D-G). These findings were consistent with earlier studies wherein other mouse strains were fed high-cholesterol diets (52; 58; 59).

Hepatic Lipid Accumulation in DKO Mice

The DKO alone modestly increased liver total lipid (Fig 1A), total neutral lipid (Fig 1B), and phospholipid (Fig 1C) in control-fed males, and even more so in control-fed females. The increases in hepatic neutral lipid were due to increased total cholesterol (Fig 1E), primarily cholesteryl ester, in both males and females (Fig 1F). The DKO significantly increased hepatic triglyceride only in control-fed female but not male mice (Fig 1G).

The DKO exacerbated the high-cholesterol diet-induced hepatic lipid accumulation, especially in females. Females had the highest hepatic levels of total lipid (Fig 1A), total neutral lipid (Fig 1B), total cholesterol (Fig 1D), free cholesterol (Fig 1E), cholesteryl ester (Fig 1F), and the glycerides: phospholipid (Fig 1C) and triglyceride (Fig 1G). The increases observed in hepatic glyceride levels were not caused by the concomitant upregulation of proteins involved in fatty acid uptake (FATP-2 or FATP-4, Fig 2C-D), downregulation of oxidation (CPT1A, Fig 2F), nor was there observed altered serum β -hydroxybutyrate (Fig 2B) and non-esterified fatty acid (Fig 2A) levels, as none of the mice expressed these changes (not shown).

In summary, the DKO induced hepatic lipid accumulation, especially in high-cholesterol fed females, and was not associated with decreased fatty acid oxidation. Instead, the DKO generally exacerbated the cholesterol diet-induced hepatic accumulation of cholesteryl ester and triglyceride, the major neutral lipid species comprising lipid droplets and the core of secreted VLDL. The majority of the increase in total cholesterol could be attributed to increased cholesteryl ester. While the overall

pattern of the liver lipid phenotype in DKO mice, especially in response to a high-cholesterol diet, was significantly altered in non-sex dependent manner, accumulation of all forms of cholesterol and triglyceride was highest in DKO females.

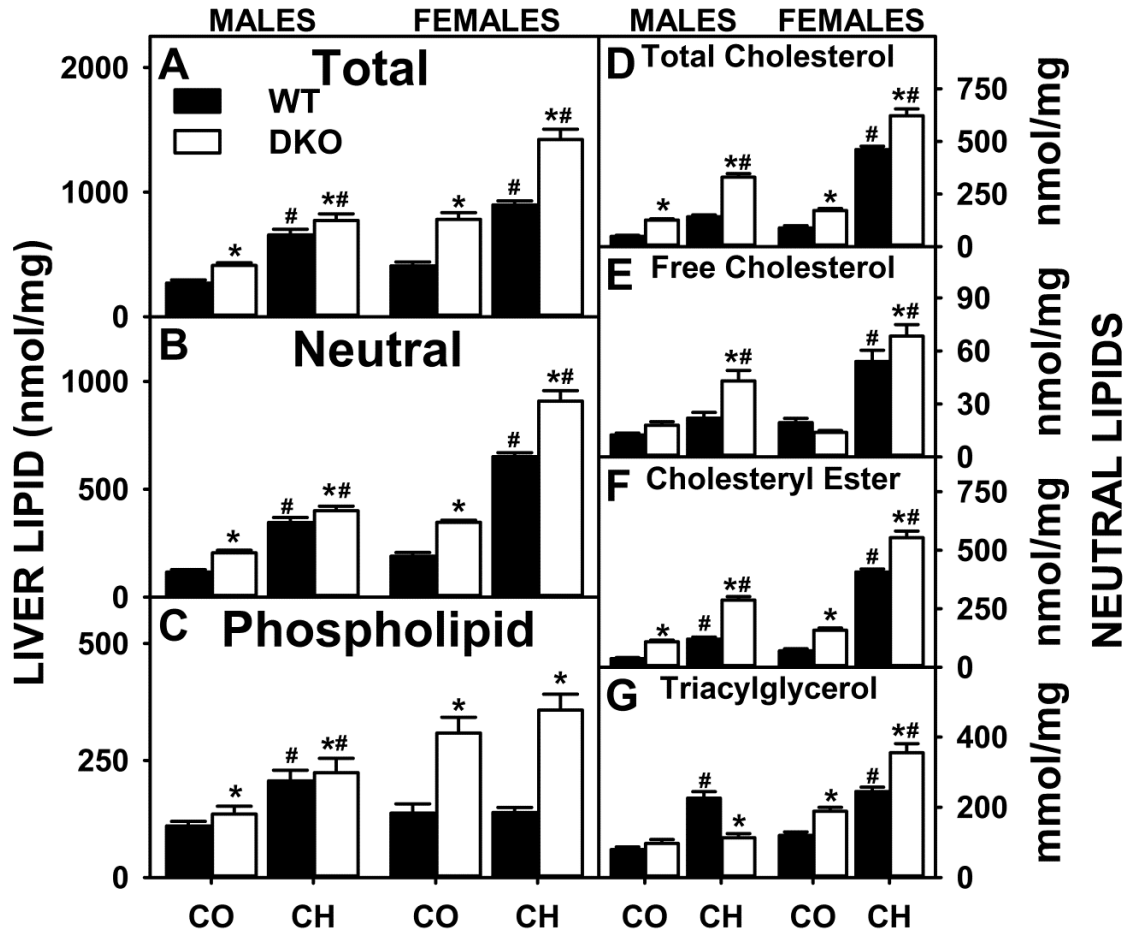


Figure 1: Effects of SCP-2/SCP-x gene ablation and cholesterol rich diet on hepatic lipid concentrations in mice. The total lipid (A), neutral lipid (B), phospholipid (C), total cholesterol (D), free cholesterol (E), cholesteryl ester (F), and triacylglycerol (G) levels from SCP-2/SCP-x^{-/-} (DKO) vs. SCP-2/SCP-x^{+/+} (WT) mice were quantified as described in MATERIALS AND METHODS. CO, control diet; CH, high-cholesterol diet; solid bars, WT; open bars, DKO mice. Values are means ± SE (n = 6-7). * *P* < 0.05 for DKO vs. WT. # *P* < 0.05 Cholesterol rich diet (CH) vs. Control diet (CO).

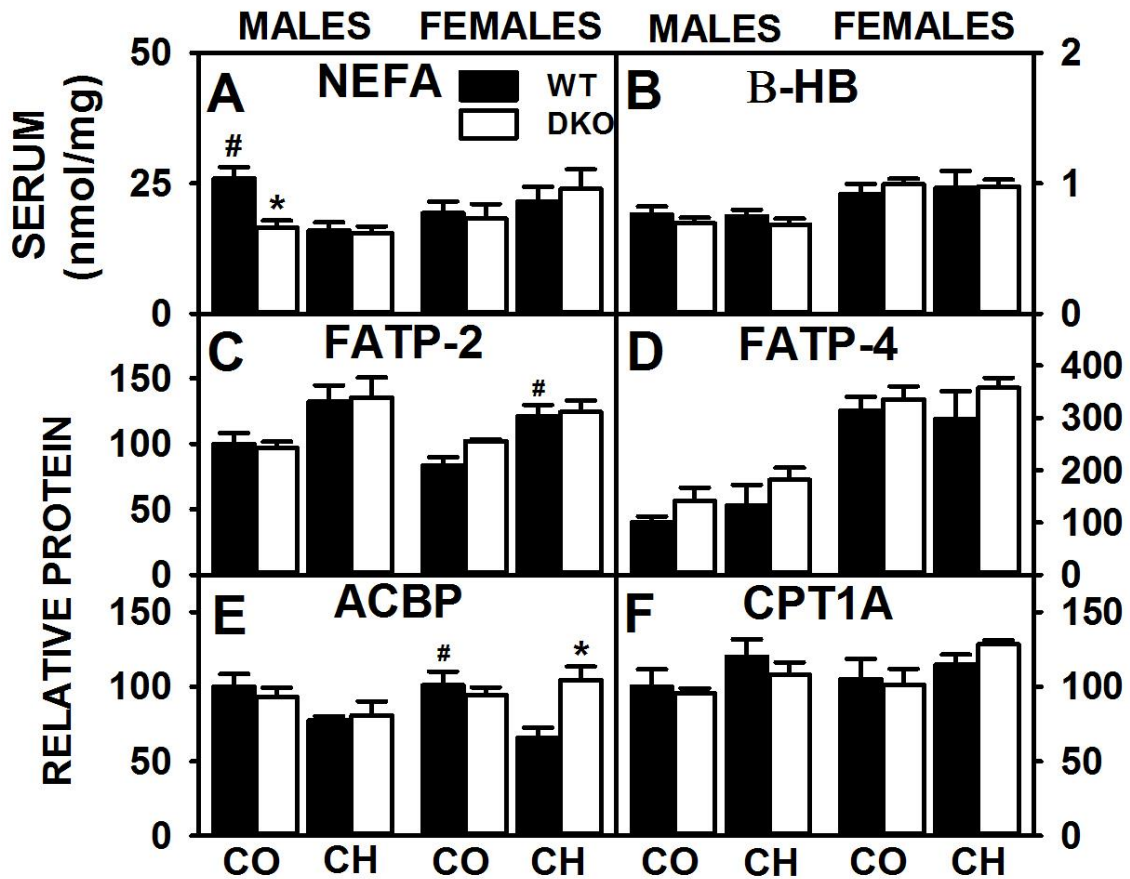


Figure 2: Effects of SCP-2/SCP-x gene ablation and cholesterol rich diet on fatty acid metabolism. Serum levels of NEFA (A) and β -HB (B) were quantified from DKO and WT mice as described in MATERIALS AND METHODS. Western blots of liver homogenates isolated from WT and DKO mice were analyzed as described in MATERIALS AND METHODS to determine relative protein levels of FATP-2 (C), FATP-4 (D), ACBP (E), and CPT1A (F) were analyzed. Cox-4 was used as a loading control to normalize protein expression. CO, control diet; CH, high-cholesterol diet; solid bars, WT; open bars, DKO mice. Values are means \pm SE (n = 5-7). * $P < 0.05$ for DKO vs. WT. # $P < 0.05$ CH vs. CO.

Serum Lipids

In contrast to the significant lipid accumulation in liver, changes in serum lipids were more modest. Serum total lipid, neutral lipid, and phospholipid were not altered in either male or female DKO mice regardless of diet (Table 3). However, a significant decrease in serum polar/neutral lipid ratio, paralleling a decrease in this ratio in liver lipids, was detected in response to the high-cholesterol diet in WT males, but not females (Table 3). The DKO prevented this decrease in serum polar/neutral lipid ratio in cholesterol fed males (Table 3). Likewise, the decreased ratio of polar/neutral lipids in livers of cholesterol fed both DKO and WT females was not reflected in serum alterations (Table 3).

Fractionation of serum neutral lipids showed that the DKO had significantly increased serum triglycerides in males but not females, on the control diet (Fig. 3D). In contrast, the high-cholesterol diet alone significantly reduced serum total and free cholesterol (Fig 3A, B), but not cholesteryl ester or triglyceride (Fig 3C, D) in male WT mice. DKO modified the tendency of cholesterol diet to increase triglyceride in males (Fig 3D). In contrast, neither DKO, high-cholesterol diet, nor both significantly altered the serum pattern of neutral lipid species in females (Fig 3A-D).

Determination of serum cholesterol distribution in the high density lipoprotein (HDL) fraction of serum lipids showed that DKO alone decreased HDL-cholesterol, but not Apo A1 or Apo A1/HDL-cholesterol ratio in control-fed males, but not females (Fig

4A,C,E). The cholesterol diet alone also decreased HDL-cholesterol but increased the Apo A1/HDL-cholesterol ratio (Fig 4A, C, E). DKO obviated the increase in Apo A1/HDL-cholesterol ratio in male, high cholesterol fed mice. In contrast, these HDL related parameters were not altered by DKO, high-cholesterol diet, or both in females.

While DKO alone did not affect the concentration of nonHDL-C, Apo B levels were significantly increased in control fed males and females (Fig 4B, D). A high cholesterol diet had little, if any, effect on serum nonHDL-C concentration in WT or DKO male or female mice; however, high cholesterol resulted in increased serum Apo B in both WT male and female mice (Fig 4B, D). There was no significant effect on the ratio of Apo B to nonHDL-C in any of the mice examined (Fig 4F). In summary, neither a high cholesterol diet nor loss of SCP-2/SCP-x had a significant effect on serum ApoA1/HDL-C or Apo B/nonHDL-C levels in male or female mice.

	MALE				FEMALE			
	WT		DKO		WT		DKO	
	CO	CH	CO	CH	CO	CH	CO	CH
Total Protein (mg/mL)	126±3	114±6	111±3	113±4	119±8	108±9	119±11	108±6
Total Lipid (mg/dL)	262±7	222±8 [#]	260±10	215±5 [#]	153±5	144±4	158±9	152±6
Neutral Lipid (mg/dL)	160±7	143±6	157±9	124±4 [#]	89±3	94±4	98±6	91±6
Phospholipid (mg/dL)	99±3	77±4 [#]	98±6	87±3	62±3	48±3 [#]	59±3	58±3*
Serum Polar/Neutral Lipid (mg/mg)	0.65±0.04	0.56±0.03	0.65±0.04	0.74±0.03*	0.73±0.04	0.53±0.04 [#]	0.63±0.02	0.69±0.06
Liver Polar/Neutral Lipid (nmol/nmol)	1.5±0.1	1.1±0.1 [#]	1.1±0.1*	0.9±0.1	1.3±0.2	0.5±0.1 [#]	1.3±0.1	0.6±0.1 [#]

Table 3: Effect of SCP-2/SCP-x gene ablation, high cholesterol diet and both together on serum lipids. The units are as follows: total protein, mg protein/mL serum; total lipid, neutral lipid, and phospholipid, mg lipid/dL serum; serum polar/neutral lipid, mg lipid/mg lipid; liver polar/neutral lipid, nmol lipid/nmol lipid. CO, control; CH, cholesterol. Values represent the mean ± SEM, n=6-7. *Genotype Effect ($P<0.05$ for DKO vs. WT within the same diet); # Diet Effect ($P<0.05$ for Control vs. Cholesterol diet within the same genotype).

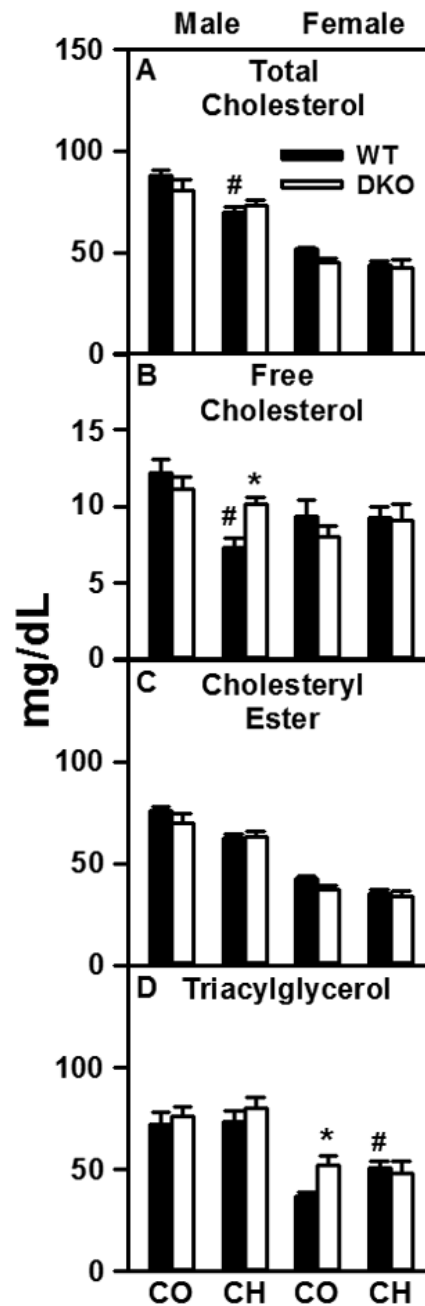


Figure 3: Effects of SCP-2/SCP-x gene ablation and cholesterol rich diet on serum cholesterol and triacylglycerol composition. Serum levels of total cholesterol (A), free cholesterol (B), cholesteryl ester (C), and triacylglycerol (D) from DKO and WT mice were quantified as described in MATERIALS AND METHODS. CO, control diet; CH, high-cholesterol diet; solid bars, WT; open bars, DKO mice. Values are means \pm SE (n = 6-7). * $P < 0.05$ for DKO vs. WT. # $P < 0.05$ CH vs. CO.

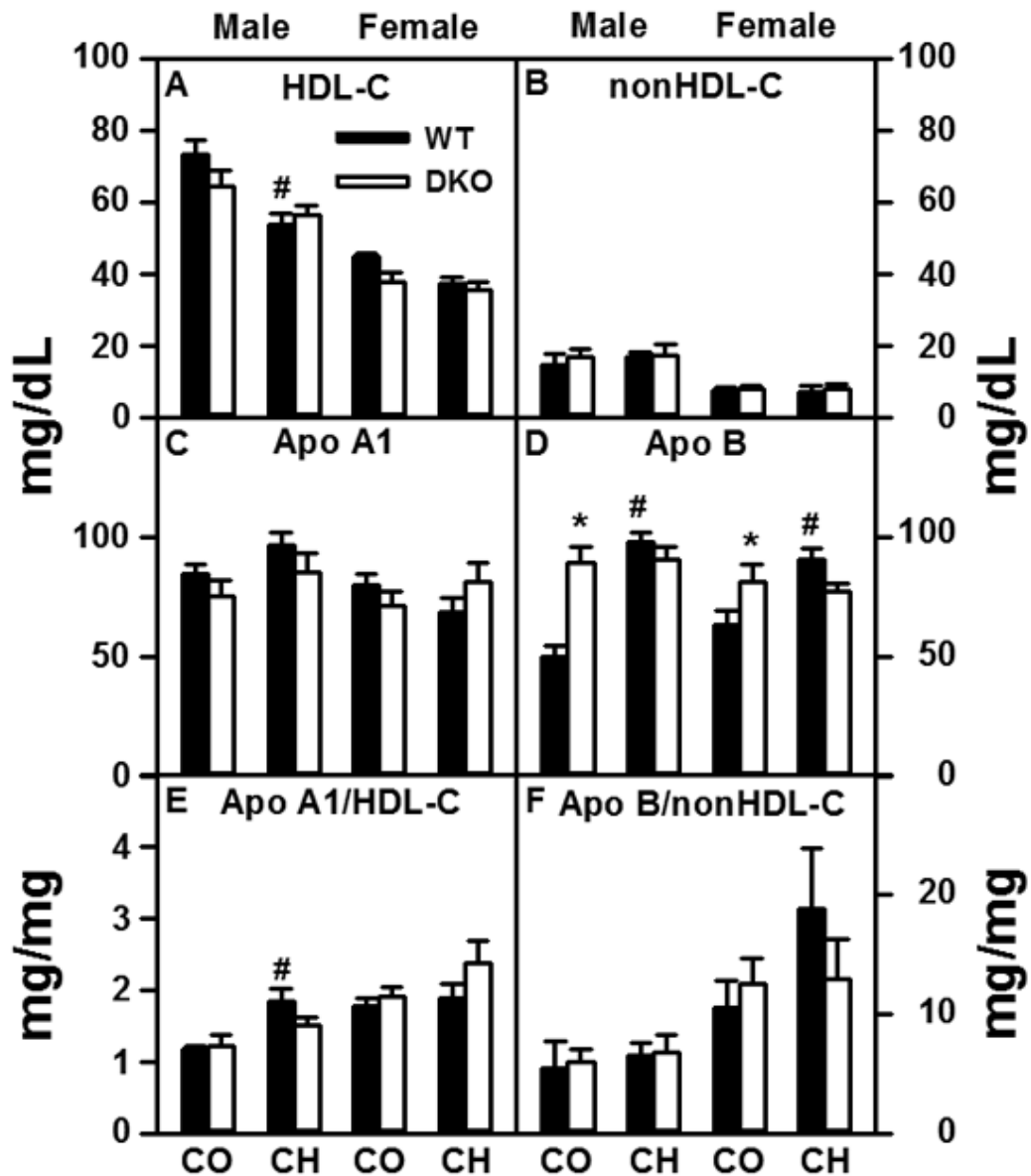


Figure 4: Effects of SCP-2/SCP-x gene ablation and cholesterol rich diet on serum lipoprotein profiles. Serum levels of HDL cholesterol (A), nonHDL cholesterol (B), Apo A1 (C) and Apo B (D) were quantified from DKO and WT mice as described in MATERIALS AND METHODS. Ratios of Apo A1/HDL-C (E) and Apo B/nonHDL-C (F) were calculated in order to elucidate particle size, reflecting atherogenicity of the particles present. CO, control diet; CH, high-cholesterol diet; solid bars, WT; open bars, DKO mice. Values are means \pm SE (n = 6-7). * $P < 0.05$ for DKO vs. WT. # $P < 0.05$ CH vs. CO.

Liver Proteins Involved in Basolateral Uptake and Storage of Cholesterol from Serum Lipoproteins

As indicated, the DKO significantly increased hepatic cholesterol accumulation, especially in cholesterol-fed females (Fig 1). Thus it was important to determine if these changes were associated with concomitant alterations in other basolateral proteins involved in serum lipoprotein-mediated cholesterol uptake/efflux from or to serum.

Hepatic accumulation of cholesterol in DKO mice was not associated with concomitant upregulation of liver basolateral membrane proteins involved in lipoprotein-mediated cholesterol uptake from serum. HDL binds to SR-B1 localized at the hepatocyte basolateral membrane for uptake of cholesterol. Overall, loss of SCP-2/SCP-x, high cholesterol diet, or both together had little effect on expression levels of SR-B1 (Fig 5A). LDL binds to LDL-R localized at the hepatocyte basolateral membrane for endocytic uptake of LDL cholesterol/cholesteryl ester. DKO decreased or tended to decrease LDL-R expression in the high-cholesterol fed males and females (Fig 5B).

Hepatic storage of cholesterol as cholesteryl ester is regulated by the opposing activities of two key proteins: the synthetic enzyme acyl CoA cholesteryl acyltransferase (ACAT2) and the degradative cholesteryl ester hydrolase/hormone sensitive lipase (*Ceh/Hsl*). DKO alone increased hepatic levels of ACAT2 in control-fed males but not females. The high cholesterol diet alone exacerbated the increase seen in WT males. (Fig 5C). However, DKO prevented this high cholesterol diet-induced increase of ACAT2 in males with little alteration in females (Fig 5D). While DKO alone had little effect on expression of *Ceh/Hsl* in either male or female control-fed mice (Fig 5C), the cholesterol

diet alone significantly increased expression of *Ceh/Hsl* in WT females, but not WT males (Fig 5C). DKO increased *Ceh/Hsl* expression in cholesterol-fed males but did not affect *Ceh/Hsl* expression levels in females (Fig 5C).

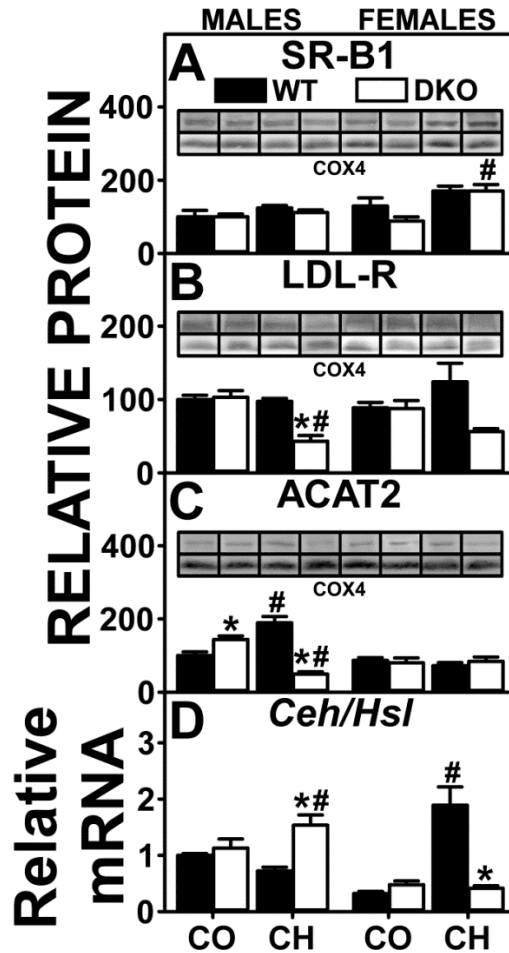


Figure 5: Analysis of key enzymes and receptors involved in the uptake and conversion of cholesterol by quantitative real time PCR (qRT-PCR) and Western blot. Western blots of liver homogenates isolated from WT and DKO mice were analyzed as described in MATERIALS AND METHODS to determine relative protein levels of SR-B1 (A), LDL-R (B), and ACAT2 (C). COX4 was used as a loading control to normalize protein expression. Insets (E-H): Representative Western blots showing relative protein expression in each mouse group. qRT-PCR was used to determine relative mRNA abundance of CEH (D). 18S rRNA was used to normalize mRNA expression levels. mRNA and protein expression levels were quantified as described in MATERIALS AND METHODS. CO, control diet; CH, high-cholesterol diet; solid bars, WT; open bars, DKO mice. Values are means \pm SE (n = 4-7). * $P < 0.05$ for DKO vs. WT. # $P < 0.05$ CH vs. CO.

In summary, the increased hepatic accumulation of cholesterol in either control- or cholesterol-fed DKO mice (Fig 1) was not associated with concomitant upregulation of SR-B1 and/or LDL-R. Accumulation of cholesteryl ester in control-fed DKO groups was associated in part with increased expression of ACAT2 in males, but not with an increase in ACAT2 or decrease in *Ceh/Hsl* in females. The DKO induced exacerbation of hepatic cholesteryl ester accumulation in females on a high cholesterol diet was associated with decreased *Ceh/Hsl* and unaltered ACAT2. Alterations in ACAT2 and *Ceh/Hsl* suggest that excess cholesterol may have remained as free cholesterol or was released from cholesteryl ester as free cholesterol.

Proteins Involved in Cytosolic Transport/Targeting of Cholesterol

While SCP-2, SCP-x and liver fatty acid binding protein (L-FABP) bind cholesterol, each differentially targets cholesterol in the hepatocyte: SCP-2 facilitates cholesterol targeting to ER for esterification and peroxisomes for oxidation; SCP-x is an exclusively peroxisomal enzyme for cholesterol oxidation to bile acids; L-FABP preferentially targets cholesterol for biliary elimination (4; 29; 57). Therefore, the impact of high-cholesterol diet, DKO, and both together on hepatic expression of these proteins was examined.

DKO resulted in complete ablation of both SCP-2 and SCP-x protein expression (Fig 6 C, D). In control-fed DKO mice, this loss was compensated only in part by concomitant upregulation of the other major bile acid binding/transport protein, L-FABP, whose expression was increased significantly in males and trended to increase

slightly in females (Fig 6E). The high cholesterol diet increased expression of L-FABP and SCP-x in WT males and increased that of SCP-2 and SCP-x (but not L-FABP) in WT females (Fig 6C-E). DKO prevented the high cholesterol diet-induced increase in hepatic L-FABP expression in males but did not alter L-FABP level in females (Fig 6E). The net effect of these changes in DKO cholesterol-fed mice was to decrease the expression of these proteins involved in cytosolic transport of cholesterol for oxidation and biliary elimination, thereby resulting in retention of cholesterol in liver.

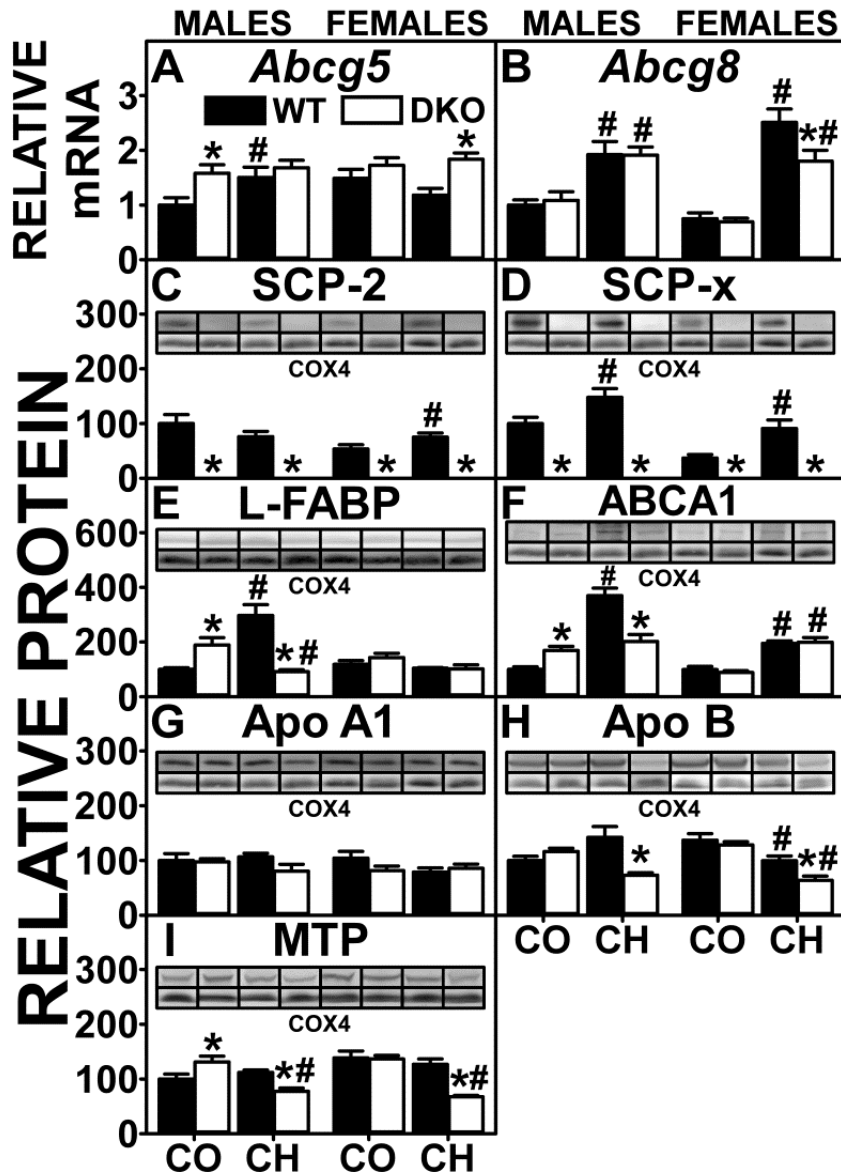


Figure 6: Analysis of key intracellular and membrane cholesterol transporters and examination of proteins involved in lipoprotein packaging by quantitative real time PCR (qRT-PCR) and Western blot. qRT-PCR was determined as in EXPERIMENTAL PROCEDURES to determine relative mRNA abundance of cholesterol efflux transporters *Abcg5* (A) and *Abcg8* (B). 18S rRNA was used to normalize mRNA expression levels. Western blots of liver homogenates isolated from WT and DKO mice were performed analyzed as in MATERIALS AND METHODS to determine relative protein levels of SCP-2 (C), SCP-X (D), L-FABP (E), ABCA1 (F), Apo A1 (G), Apo B (H), and MTP (I). COX4 was used as a loading control to normalize protein expression. Insets (E-H): Representative Western blots showing relative protein expression in each mouse group. CO, control diet; CH, high-cholesterol diet; solid bars, WT; open bars, DKO mice. Values are means \pm SE (n = 4-7). * $P < 0.05$ for DKO vs. WT. # $P < 0.05$ CH vs. CO.

Hepatic Proteins Involved in Secretion of Cholesterol and Other Lipids Into Serum

Assembly of neutral lipid-loaded nascent VLDL for secretion into serum requires the concerted action of L-FABP (and/or SCP-2) (13; 32; 47; 48; 69; 79; 108), MTP (90) and Apo B (90). Therefore, the possibility that the DKO-associated hepatic lipid accumulation might be associated with concomitant downregulation of these hepatic proteins was examined.

First, Both SCP-2 and L-FABP were increased by the high cholesterol diet in WT males, but only SCP-2 and SCP-x were increased in WT females (Fig 6C-E). While the DKO alone increased L-FABP in males, this was not observed in females (Fig 6E). DKO decreased (males) or did not alter (females) expression of L-FABP in cholesterol-fed mice (Fig 6E). Second, neither DKO alone nor high cholesterol diet alone significantly altered Apo B expression (Fig 6H). In contrast, hepatic levels of Apo B were markedly reduced in high cholesterol fed DKO mice (Fig 6H). Third, the cholesterol diet alone did not significantly alter MTP expression in males or females (Fig 6I). However, DKO did significantly decrease MTP expression in both male and female high cholesterol-fed mice (Fig 6I).

Thus, hepatic lipid accumulation (cholesterol ester, phospholipid, and triglyceride) in high cholesterol-fed DKO mice was associated not only with absence of SCP-2 and SCP-x but also with reduced hepatic levels of L-FABP (males only) as well as reduced levels of Apo B and MTP in both males and females. As shown in the following sections, the reduced levels of MTP in high cholesterol fed DKO mice were

associated with increased hepatic levels of SREBP1 and SREBP2 proteins, both of which are known to negatively influence transcription of *Mttp*.

Nuclear Receptors Involved in Hepatic De Novo Synthesis of Fatty Acids

Both SREBP1 and SREBP2 regulate transcription of enzymes and transporters involved in hepatic accumulation of cholesterol and glycerides (88; 90; 106; 116). Thus, hepatic expression and transcription of *Srebp1* and *Srebp2* as well as their target genes (*Acc1*, *Acc2*, *Fas*) in de novo fatty acid synthesis were examined.

Although the high-cholesterol diet increased transcription of *Srebp1* (Fig 7C), this did not translate to increased levels of mature nuclear 68 kDa SREBP1 protein (Fig 7A) or its larger precursor pre-SREBP1 (endoplasmic reticulum bound) (Fig 7B). In contrast, high cholesterol diet significantly increased hepatic levels of SREBP2 protein, both the mature 68 kDa SREBP2 and pre-SREBP2 forms (Fig 8B, C). Consistent with high cholesterol induced increase in SREBP2 protein levels, the expression of lipogenic target genes *Acc1* (Fig 6D), *Fas* (Fig 7F), and in the case of females also *Acc2* (Fig 7E) was increased.

In contrast, the DKO alone induced hepatic glyceride accumulation that was associated with increased levels of SREBP1 protein (Fig 7A), but not pre-SREBP1 (Fig 7B), despite unaltered *Srebp1* transcription (Fig 7C). Even more so, the DKO alone induced hepatic glyceride accumulation was associated with increased hepatic levels of mature SREBP2 protein (Fig 8B) and, in the case of males also pre-SREBP2 (Fig 8C), both of which were associated with significantly increased transcription of *Srebp2* (Fig

8A). Consistent with increased SREBP1 and SREBP2 protein, DKO alone increased transcription of target genes *Acc1* in both males and females (Fig 7D) as well as also *Fas* in females (Fig 7F).

While the high cholesterol diet did not exacerbate increases in mature SREBP1 protein in livers of DKO mice (Fig 7A), pre-SREBP1 protein was increased in males but not females (Fig 7B). However, the increased protein level was not associated with altered *Srebp1* transcription (Fig 7A). Likewise, high cholesterol diet did not further exacerbate the DKO induced increase in hepatic protein levels of SREBP2 (Fig 8B) and pre-SREBP2 (Fig 8C) or transcription of *Srebp2* (Fig 8A). Consistent with these findings, high-cholesterol also did not further increase the DKO induced transcription of *de novo* fatty acid synthesis target genes (Fig 7D-F).

In summary, altered levels of SREBP1 and SREBP2 nuclear regulatory proteins as well as their target genes for *de novo* fatty acid synthesis contributed at least in part to hepatic lipid accumulation in DKO, high cholesterol-fed and DKO/high cholesterol-fed mice.

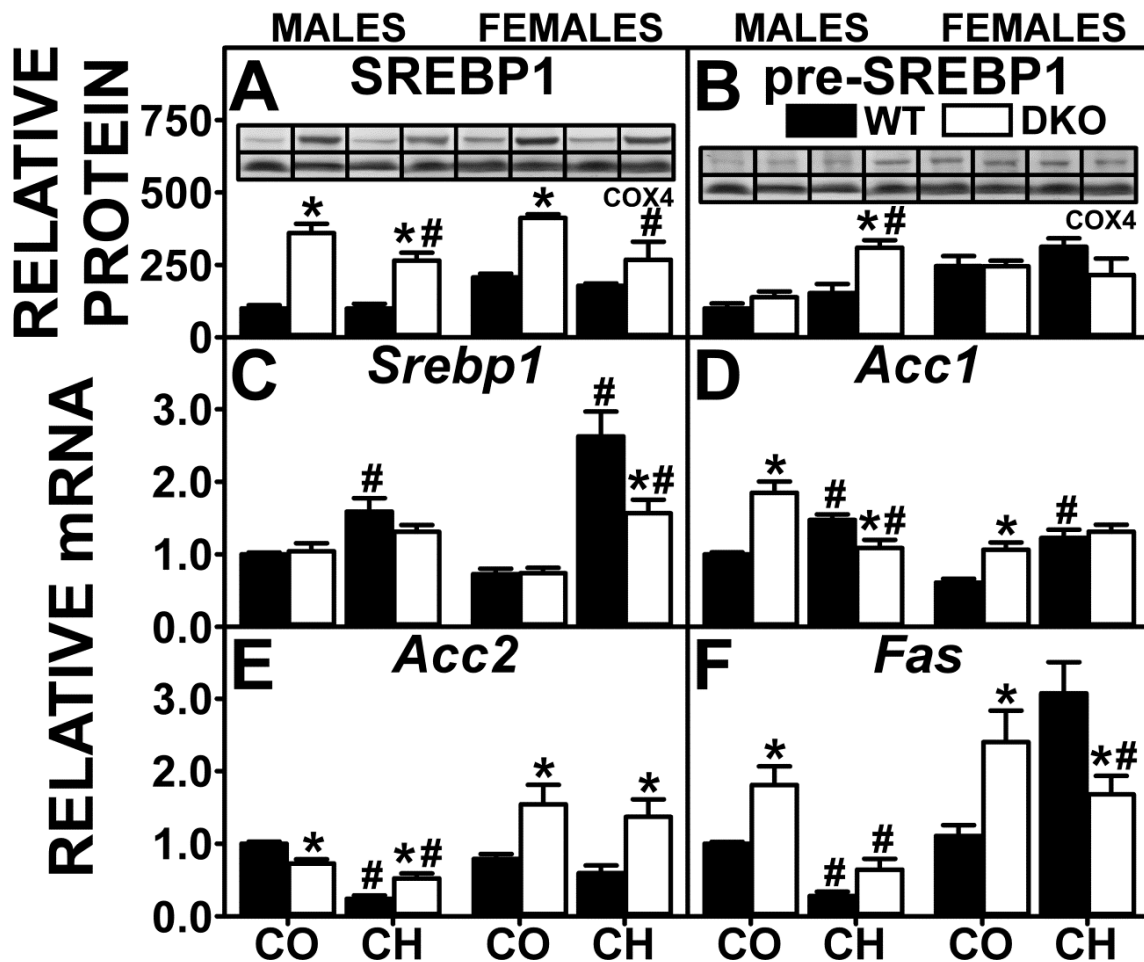


Figure 7: Effect of SCP-2/SCP-X gene ablation and cholesterol rich diet on key regulators of fatty acid biosynthesis. Western blots of liver homogenates isolated from WT and DKO mice were analyzed to determine relative protein levels of the 68kDa SREBP1 (A) and 125kDa pre-SREBP1 (B). COX4 was used as a loading control to normalize protein expression. qRT-PCR was used to determine relative mRNA abundance of *Srebp1* (C), *Acc1* (D), *Acc2* (E), and *FAS* (F). 18S rRNA was used to normalize mRNA expression levels. mRNA and protein expression levels were quantified as described in was determined as in MATERIALS AND METHODS. Insets (E-H): Representative Western blots showing relative protein expression in each mouse group. CO, control diet; CH, high-cholesterol diet; solid bars, WT; open bars, DKO mice. Values are means \pm SE (n = 4-7). * $P < 0.05$ for DKO vs. WT. # $P < 0.05$ CH vs. CO.

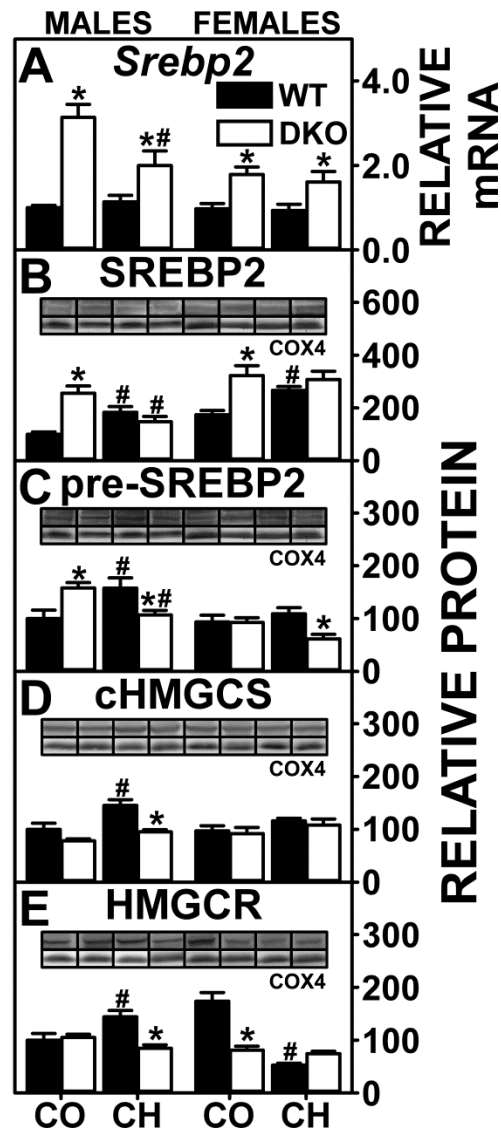


Figure 8: Effect of SCP-2/SCP-X gene ablation and cholesterol rich diet on key regulators of cholesterol biosynthesis. qRT-PCR was used to determine relative mRNA abundance of *Srebp2* (A). 18S rRNA was used to normalize mRNA expression levels. Western blots of liver homogenates isolated from WT and DKO mice were analyzed to determine relative protein levels of SREBP2 (68kDa, B) and pre-SREBP2 (125kDa, C), cHMGCS (D) and HMGCR (E). COX4 was used as a loading control to normalize protein expression. mRNA and protein expression levels were quantified as described in MATERIALS AND METHODS. Insets (E-H): Representative Western blots showing relative protein expression in each mouse group. CO, control diet; CH, high-cholesterol diet; solid bars, WT; open bars, DKO mice. Values are means \pm SE (n = 4-7). * $P < 0.05$ for DKO vs. WT. # $P < 0.05$ CH vs. CO.

Nuclear Receptors Involved in Hepatic Lipoprotein Secretion and De Novo Synthesis of Cholesterol

SREBP2, but much less so SREBP1, specifically regulates transcription of enzymes and transporters involved in hepatic accumulation of cholesterol (88; 90; 106; 116). Therefore, the possibility that DKO induced hepatic cholesterol accumulation in cholesterol-fed mice was associated with altered SREBP2 transcription or protein expression was examined.

High cholesterol diet alone induced cholesterol accumulation that was associated with increased levels of SREBP2 protein in both males and females (Fig 8B) as well as pre-SREBP2 protein in males (Fig 8C), while *Srebp2* transcription was unaltered (Fig 8A). Consistent with cholesterol-induced increase in SREBP1 protein, expression of several SREBP2 target gene products such as proteins, cHMGCS (Fig 8D) and HMGCR, (Fig 8E) were increased in males but not females. In contrast, levels of other SREBP2 target genes such as LDL-R (Fig 5B) and SR-B1 (Fig 5A) were unaltered by high-cholesterol diet in both sexes.

DKO alone increased hepatic levels of SREBP2 protein in both males and females (Fig 8B) as well as also pre-SREBP2 protein in males (Fig 8C). The increased SREBP2 protein correlated with significantly increased transcription of *Srebp2* (Fig 8A). However, protein levels of SREBP2 target genes such as cHMGCS (Fig 8D), HMGCR (Fig 8E), LDL-R (Fig 5B), or SR-B1 (Fig 5A) were not increased. DKO did not further increase high-cholesterol diet induced levels of SREBP2 proteins or mRNAs (Fig 8A-C). Likewise, DKO did not increase protein levels of SREBP2 target genes such as

cHMGCS (Fig 8D), HMGCR (Fig 8E), LDL-R (Fig 5B), or SR-B1 (Fig 5A) in high-cholesterol fed mice.

In summary, altered expression of key nuclear regulatory proteins in transcription of *Srebp2* as well as its translation/accumulation as SREBP2 protein in part contributed to hepatic lipid accumulation in the DKO high cholesterol-fed and the DKO control-fed mice.

Canalicular Membrane Proteins Involved in Biliary Excretion of Cholesterol

L-FABP, more so than SCP-2, is involved in hepatic uptake and cytosolic transfer of HDL-derived cholesterol to bile canaliculus for secretion into bile (57). Biliary levels of cholesterol were unaltered except in control- (decreased) and cholesterol-fed (increased) DKO males (Fig 9D). Therefore, the impact of DKO and high cholesterol-diet on expression of key canalicular membrane transporters (*Abcg5*, *Abcg8*) in biliary cholesterol excretion was determined.

The high-cholesterol diet alone increased transcription of *Abcg5* in males, but not females (Fig 6A), but increased transcription of *Abcg8* in both males and females (Fig 6B). DKO alone also increased transcription of *Abcg5* in males, but not females (Fig 6A), while transcription of *Abcg8* in either sex was unaltered (Fig 6B). DKO did not further exacerbate the high-cholesterol diet induced transcription of *Abcg5* in males, but increased that in females (Fig 6A), and did not increase transcription of *Abcg8* in either males or females (Fig 6B).

While ABCG5 and ABCG8 proteins operate as heterodimer pairs to mediate excretion of cholesterol into bile, DKO did not induce concomitant upregulation of both *Abcg5* and *Abcg8*. Nevertheless the increased biliary cholesterol in DKO high cholesterol-fed males, correlated with a significant increase in biliary bile acid (Fig 9C), the driving force of cholesterol secretion into bile (84; 89; 115).

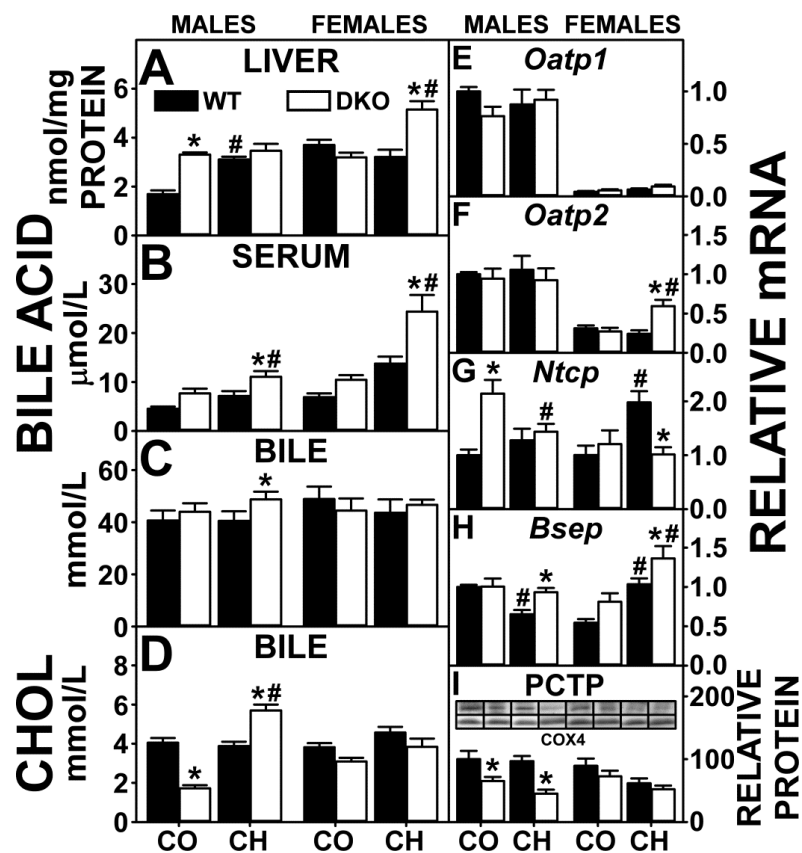


Figure 9: Bile acid levels and hepatic expression of key proteins in bile acid reuptake and biliary excretion. Liver (A), Serum (B), Biliary (C) bile acids and biliary cholesterol (D) levels were quantified as in MATERIALS AND METHODS. qRT-PCR was performed as in MATERIALS AND METHODS to determine relative mRNA abundance of OATP1 (E), OATP2 (F), NTCP (G), and BSEP (H). 18S rRNA was used to normalize mRNA expression levels. Western blots of liver homogenates isolated from WT and DKO mice were obtained and analyzed as in MATERIALS AND METHODS to determine relative protein level of PCTP (I). COX4 was used as a loading control to normalize protein expression. Insets (E-H): Representative Western blots showing relative protein expression in each mouse group. CO, control diet; CH, high-cholesterol diet; solid bars, WT; open bars, DKO mice. Values are means \pm SE (n = 4-7). * $P < 0.05$ for DKO vs. WT. # $P < 0.05$ CH vs. CO.

Hepatic, Serum and Biliary Bile Acid Level

The DKO impact on bile acid levels was sex- and high cholesterol diet dependent. This KO induced a twofold accumulation of bile acids in liver and trended towards an increase in serum bile acids but not biliary bile acids in control-fed males but not females (Fig 9A-C). The high cholesterol diet alone significantly increased bile acid accumulation in liver, but not serum or bile, of males without significantly altering those in females (Fig 9A-C). DKO induced bile acid accumulation in serum and biliary bile while retaining levels of bile acid constant in livers of high cholesterol fed males (Fig 9A-C). In contrast, DKO induced bile acid accumulation in liver and serum while maintaining that in bile constant in high cholesterol-fed females (Fig 9A-C).

Thus the DKO elicited bile acid retention in liver and serum in both males and female and increased biliary bile acid accumulation only in high cholesterol-fed males, wherein biliary cholesterol levels also increased. These data were consistent with canalicular secretion of bile acid driving biliary cholesterol secretion (84; 89; 115).

Expression of Proteins Involved in Hepatic Bile Acid Transport

Hepatic expressions of basolateral membrane (*Oatp1*, *Oatp2*, *Ntcp*) and canalicular membrane (*Bsep*) bile acid transporters were examined. Expression of *Oatp1* (Fig 9E) and *Oatp2* (Fig 9F) was unaltered in male DKO mice. While expression of *Ntcp* (Fig 9G) was increased in control-fed DKO mice and in the WT males on a high cholesterol diet, these increases were not sufficient to reduce the elevated bile acid levels in serum (Fig 9B). Similarly, DKO alone did not alter liver transcription levels of *Oatp1*,

Oatp2, or *Ntcp* in control-fed females (Fig 9E-G). The high cholesterol diet alone increased only *Ntcp* in WT females (Fig 9G) and only *Oatp2* in DKO females (Fig 9F). In general, DKO, high cholesterol diet, or both did not reduce expression of these transporters, thereby reducing reuptake of bile acid from serum, in order to explain the increased serum bile acids observed in either sex.

In contrast, the increased serum, but not hepatic, bile acid levels in control-fed male and female DKO mice were attributable in part to altered expression of cytosolic bile acid transport proteins. The DKO resulted in complete absence of both SCP-2 and SCP-x (Fig 6C, D), key proteins in cytosolic bile acid transport as well as bile acid synthesis. In control-fed DKO mice, this loss was compensated in part by concomitant upregulation of the other major bile acid binding/transport protein, L-FABP, whose expression was increased significantly in males and trended to increase slightly in females (Fig 6E). The high cholesterol diet alone increased expression of L-FABP and SCP-x in WT males and increased that of SCP-2 and SCP-x (but not L-FABP) in WT females (Fig 6C-E). The DKO prevented the cholesterol diet-induced increase in hepatic L-FABP expression in males but did not alter L-FABP level in females (Fig 6E). Taken together, the net effect was to decrease the expression of cytosolic proteins involved in hepatocyte uptake/cytosolic transport of bile acids—thereby overall favoring retention of bile acids in serum.

The unaltered biliary bile acid levels in control-fed WT groups (Fig 9C) were consistent with unaltered expression of canalicular bile acid transporter *Bsep* (Fig 9H). While the high cholesterol diet alone decreased *Bsep* expression in WT males and increased that in females, these changes were insufficient to alter bile acid levels in bile (Fig 9C). DKO prevented the cholesterol-induced increase in *Bsep* in males, but exacerbated the increased *Bsep* in females (Fig 9H). Alterations observed in *Bsep* did not consistently correlate with increased biliary bile acids (Fig 9C).

Interestingly, DKO significantly decreased hepatic expression of PCTP in DKO males and trended to decrease that in DKO females fed either the control or high cholesterol diet (Fig 9I). PCTP is the major cytosolic transport protein of phosphatidylcholine, also needed for formation of bile. While this change did not lead to decreased bile acid levels, it may have contributed in part to hepatic retention of phospholipids (Fig 1C) and/or bile acids (Fig 9A).

Taken together, these data showed that the bile acid and biliary lipid phenotype of DKO mice was in large part associated with the loss of SCP-2 and SCP-x, but less so with altered regulation of other membrane and cytosolic proteins involved in bile acid transport and bile formation.

Expression of Enzymes Involved in Hepatic Bile Acid and Cholesterol Synthesis

Mice and humans exhibit marked sex- dependent differential expression of the rate limiting enzymes in the primary and secondary pathways for bile acid synthesis. Expression of CYP7A1 (rate limiting enzyme in the primary bile acid synthesis

pathway) and CYP27A1 (rate limiting enzyme in the alternate pathway of bile acid synthesis) were several fold higher in female mice than male mice under all conditions examined (Fig 10A, B).

Neither DKO alone, high cholesterol diet alone, nor did both together impact expression of CYP7A1 in either sex (Fig 10A). In contrast, DKO alone, but not high cholesterol diet alone or both together, increased expression of the alternate pathway enzyme CYP27A1 in males, while decreasing that in females (Fig 10B).

Taken together, these data indicated that higher total bile acid level (liver, serum, bile) of control-, but not high cholesterol-fed, females were associated with higher hepatic expression of key bile acid synthetic enzymes CYP7A1 and CYP27A1. However, higher total bile acid level (liver, serum, bile) in cholesterol-fed DKO males and females did not appear to be due to further increased expression of either CYP7A1 or CYP27A1.

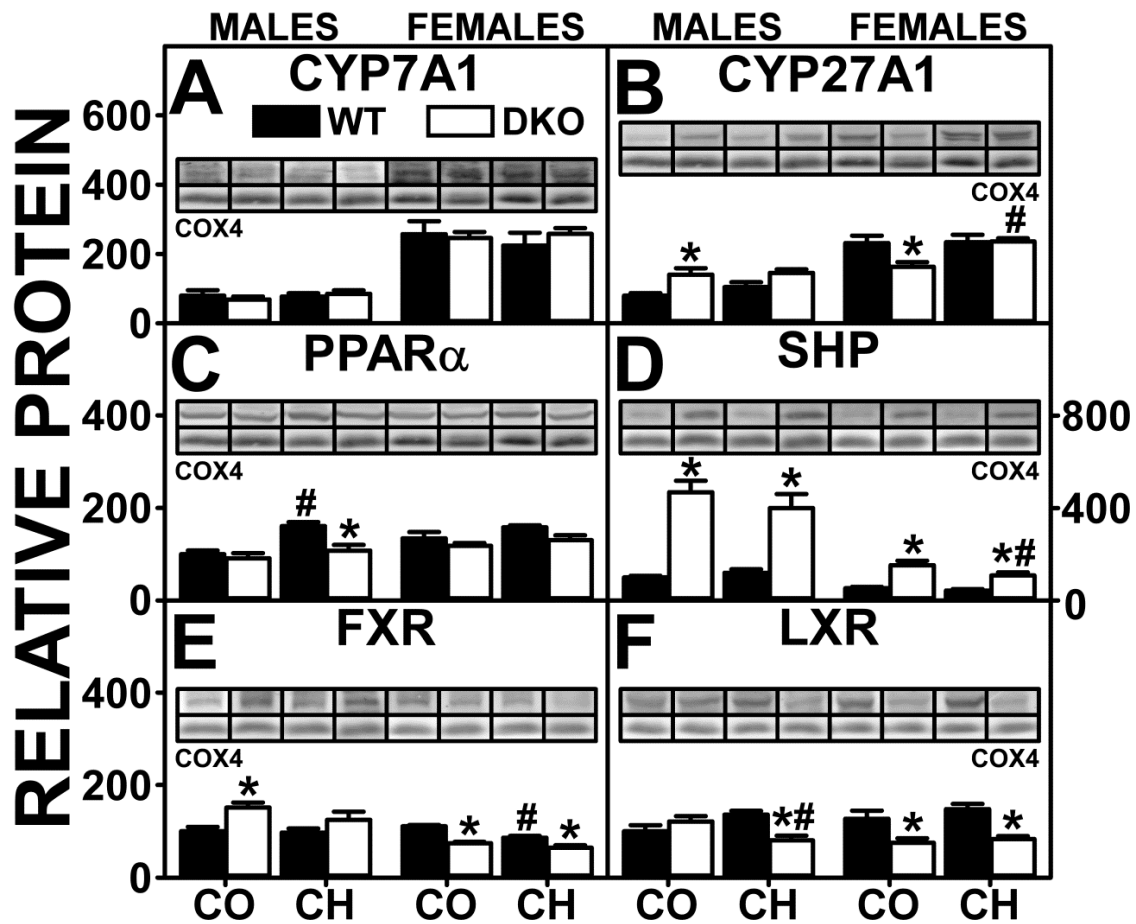


Figure 10: Effect of SCP-2/SCP-x gene ablation and cholesterol rich diet on proteins and transcription factors involved in cholesterol synthesis and oxidation to bile acids. Western blots of homogenates isolated from the livers of DKO and WT mice were analyzed to determine relative protein levels of CYP7A1 (A), CYP27A1 (B), PPAR α (c), SHP (D), FxR (E), and LxR (F). COX4 was used as a loading control to normalize protein expression. Expression levels were quantified as described in MATERIALS AND METHODS. Insets: Representative Western blots showing relative protein expression in each mouse group. CO, control diet; CH, high-cholesterol diet; solid bars, WT; open bars, DKO mice. Values are means \pm SE (n = 5-7). * $P < 0.05$ for DKO vs. WT. # $P < 0.05$ CH vs. CO.

Nuclear Receptors Involved in Hepatic Bile Acid Synthesis

Neither sex, DKO alone, nor DKO/high cholesterol diet together significantly increased expression of PPAR α (Fig 10C), a nuclear receptor reported to inhibit and in other cases stimulate expression of bile acid synthetic enzymes CYP7A1 and CYP27A1 (53; 54; 89). However, the cholesterol diet alone increased PPAR α expression in WT males and tended to increase in females (Fig 10C).

The nuclear receptor inhibitor SHP was significantly increased in all DKO groups (Fig 10D), while expression of LXR, a key nuclear receptor which induces transcription of CYP7A1 (89), was decreased in all DKO groups except control-fed males (Fig 10F). However, the expression of CYP7A1 was not decreased in control-fed DKO males (Fig 10A). The increased SHP in DKO males was associated with increased FXR (Fig 10E), a known SHP inducer (89). However, the decreased FXR levels in DKO females (Fig 10E) accounted in part for the smaller increase in SHP (Fig 10D).

In summary, altered expression of nuclear receptors regulating hepatic bile acid synthesis did not appear to account for sex, DKO, and diet differences in expression of key enzymes in bile acid synthesis (CYP7A1, CYP27A1). These findings were consistent with expression of these enzymes being regulated more by availability of ligand activators in the nucleus than expression levels of nuclear receptors in cholesterol and bile acid synthesis.

SUMMARY AND DISCUSSION

Since mammals have a limited ability to eliminate excess cholesterol, primarily via bile, cholesterol homeostasis is closely regulated by a delicate balance between hepatic cholesterol uptake from serum lipoproteins via plasma membrane receptors, *de novo* synthesis in the ER, feedback regulation of *de novo* synthesis via nuclear receptors, and by elimination via the bile canaliculus. Unclear, however, is how the very poorly soluble cholesterol (critical micellar concentration near 30 nM) is rapidly transported and targets within the hepatocyte in these processes. For example, the half-time for hepatic clearance of HDL cholesterol into bile is only 1-3 min (35; 86; 87; 126). *In vitro* studies with purified membranes demonstrated that spontaneous and vesicular cholesterol movement are too slow since half times are days-weeks and greater than 15 minutes, respectively (3; 8; 27; 28; 30; 31; 64; 96; 97; 99). Increasing findings *in vitro* and with cultured cells indicate potential roles of the intracellular binding proteins SCP-2, SCP-x, and L-FABP that bind, transfer, and/or target cholesterol within hepatocytes for esterification, oxidation to bile acids, and/or biliary excretion (16; 126). To study the physiological significance of these findings, murine SCP-2 has been increased by overexpression (2; 5; 125) and decreased by SCP-2 antisense treatment (83) or ablation (25; 50; 104), while L-FABP has only been ablated (60; 62). While the effect of L-FABP gene ablation on hepatic phenotype of both male and female mice has been examined in response to a high cholesterol diet (58; 59), almost nothing is known about the impact of SCP-2/SCP-x expression in the context of high dietary cholesterol for either sex. While

understandably physiologically complex, the findings presented herein provided the following new insights.

DKO Effect on Whole Body Phenotype

The DKO affected whole body phenotypes in both a sex- and high cholesterol diet-independent fashion. While DKO did not alter food consumption in either sex, body weight (BW) gain and BW gain/food consumption were decreased in females but not males regardless of diet. Other whole body phenotype parameters were not altered. Conversely, SCP-2 overexpression exacerbated BW gain in females without altering that in males (5). In contrast, high cholesterol dietary stress alone did not significantly alter whole body phenotype of either males or females. Thus, SCP-2 presence versus absence significantly impacted whole body phenotype of females more than that of males.

DKO Elicited Hepatic Accumulation of Cholesterol

The DKO resulted in loss of both SCP-2 and SCP-x and elicited hepatic accumulation of total cholesterol, primarily as cholesteryl ester, in livers of control and high cholesterol-fed mice regardless of sex. This effect was attributed to loss of SCP-2 and in male control-fed DKO mice as well as to the upregulation of L-FABP as shown herein (Fig 6E) and earlier (110). Ablating only SCP-x alone did not increase hepatic cholesterol and cholesteryl ester or alter expression of SCP-2 and L-FABP in male and female mice (6). Interestingly, SCP-2 overexpression increased hepatic accumulation of cholesteryl ester in males and females concomitant with upregulation of L-FABP in

females but not males (5). Likewise, hepatic adenoviral SCP-2 overexpression trended to increase hepatic cholesteryl ester accumulation in males, but L-FABP was not measured (2; 125). These findings would indicate that not only loss of SCP-2 but also concomitant upregulation of L-FABP was a significant contributor to the hepatic cholesterol accumulation in control-fed mice. Consistent with the latter possibility, L-FABP upregulation in cultured primary hepatocytes from DKO mice significantly increased hepatocyte uptake of HDL cholesterol (112). Although SCP-2 is more potent than L-FABP in stimulating cholesterol transfer and microsomal ACAT-mediated cholesterol esterification *in vitro* (15; 23; 24; 45; 68; 74; 79), hepatic L-FABP levels are normally greater than tenfold higher than those of SCP-2 (94; 110).

Finally, in control-fed males, but not females, the DKO-induced hepatic cholesteryl ester accumulation was also attributed in part to increased expression of ACAT2, the key ER protein responsible for esterifying cholesterol. Since the DKO did not significantly impact expression of *Ceh/Hsl*, the enzyme hydrolyzing cholesteryl ester to free cholesterol, the increased cholesteryl ester was not due to decreased *Ceh/Hsl*. Taken together, these findings were consistent with DKO-induced hepatic cholesterol and cholesteryl ester accumulation being associated in part with loss of SCP-2 concomitant with upregulation of L-FABP and/or ACAT2 at least in males.

The DKO-induced hepatic cholesterol accumulation was not due to concomitant induction of *Srebp2* transcription or increased translation into pre-SREBP2 protein and release of mature SREBP2 protein. SREBP2 is a nuclear receptor protein that is released from ER in response to low cholesterol levels therein followed by transfer into nuclei to

induce expression of target genes (36; 106; 116). Since SCP-2, and less so L-FABP, are very active in mediating cholesterol transfer from lysosomes and plasma membranes to ER (3; 8; 23; 24; 27; 28; 92), these data suggest a potential role for SCP-2 and less so L-FABP in mediating transfer of cholesterol to the ER cholesterol-sensing protein SCAP. In this scenario, loss of SCP-2 would reduce delivery of cholesterol to ER, reduce cholesterol available to SCAP in ER, and thereby induce processing of pre-SREBP2 to cleave/release mature SREBP2 protein for transfer to nuclei and activation of SREBP2 target genes in cholesterol uptake and *de novo* synthesis. Surprisingly, therefore, the expression of most SREBP2 target genes examined was unaltered or decreased in DKO females (LDL-R, SR-B1, cHMGCS, MTP, HMGCR) while changes in DKO males were modest. While the basis for the muted response of target genes to increased SREBP2 protein in DKO mice is not completely clear, altered expression of inhibitory miRNA or antagonistic nuclear regulatory proteins as well as increased degradation or posttranslational modifications may contribute. Future studies will address these issues which are beyond the scope of this thesis work.

DKO Significantly Potentiated the Induced Hepatic Cholesterol Accumulation Observed in Mice fed a High Cholesterol Diet

The DKO significantly potentiated the high cholesterol diet-induced hepatic accumulation of free and esterified cholesterol. In DKO males only, this effect was associated not only with loss of SCP-2 and SCP-x, but also with concomitant down regulation of L-FABP, the key protein involved in hepatic biliary efflux of HDL

cholesterol (57). While it was expected that SCP-2 overexpression in male mice would elicit the opposite effect, SCP-2 overexpression also potentiated cholesterol diet-induced cholesterol and cholesteryl ester accumulation concomitant with increased SCP-2 and/or concomitant downregulation of L-FABP in male mice (5). Reasons for the discrepancy may relate to the differences in mouse strains used in the overexpression versus gene ablation studies. It is important to note that although the DKO also increased *Srebp2* mRNA and SREBP2 protein in cholesterol-fed mice, this increase did not exceed that elicited by DKO alone in control-fed mice. Likewise, this increase in SREBP2 protein did not further induce expression SREBP2 target gene products (LDL-R, SR-B1, cHMGCS, HMGCR) beyond that elicited by DKO alone in control-fed mice. An exception was the fact that the DKO did reduce the hepatic protein level of MTP in cholesterol-fed but not control-fed mice since MTP is a known target gene whose transcription is inhibited by SREBP2. Finally, DKO exacerbation of cholesterol diet-induced hepatic cholesterol accumulation was associated in part with decreased *Ceh/Hsl* in females concomitant with unaltered ACAT2 level. Thus DKO exacerbation of the cholesterol diet-induced accumulation of hepatic cholesterol was associated primarily with loss of SCP-2, downregulation of L-FABP, and reduced level of MTP and downregulation of *Ceh/Hsl*.

DKO Increased Hepatic Accumulation of Glycerides

The DKO alone increased hepatic, but not serum, accumulation of glycerides: phospholipid and triacylglycerides. Livers of control-fed DKO mice exhibited higher

levels of phospholipid and triglyceride levels in both sexes. Serum lipids were largely refractory to these changes with the exception of increased triglycerides in males. The increased hepatic accumulation of glycerides (phospholipids, triglycerides) was associated with concomitant upregulation of L-FABP at least in males. Like SCP-2 (21; 46; 49; 71; 101; 108), L-FABP also binds long chain fatty acids (LCFA) (42; 55; 85; 119), stimulates LCFA uptake (66; 67; 70; 72; 73; 82; 121), and enhances LCFA cytosolic transport (70; 118). Further, L-FABP facilitates LCFA/LCFA-CoA targeting toward both the ER for esterification by GPAT (13; 47-49; 100) as well as toward oxidative organelles (mitochondria, peroxisomes) for degradation, as shown *in vitro*, in cultured cells and hepatocytes, and *in vivo* (7; 12; 39; 60). The balance between these opposing pathways is apparently determined by LCFA load (4). Further, while the DKO-induced hepatic glyceride accumulation was not associated with any change in nuclear receptor *Srebp1* mRNA level, western blotting showed that translation and release as mature SREBP1 protein was increased, as was the expression of SREBP1 lipogenic target genes (*Acc1*, *Fas*, and/or *Acc2*). In liver, the primary SREBP1 isoform is SREBP1c, and overexpression of SREBP1c induces transcription of multiple lipogenic genes (*Acc1*, *Acc2*, *Fas*) but not cholesterogenic (*Hmgcs*, *Hmgcr*) genes (106; 116). While the *Acc1* and *Fas* gene products are involved in *de novo* fatty acid synthesis, the *Acc2* gene product produces malonyl CoA at the mitochondrial membrane where the malonyl CoA then inhibits CPT1, the rate limiting step in fatty acid oxidation—thus increasing fatty acid availability for esterification.

Consistent with hepatic glyceride accumulation in DKO mice being associated with increased SREBP1 protein level, polymorphisms in SREBP1 have been associated with nonalcoholic fatty liver disease in humans (36; 75). In addition, DKO-induced upregulation of SREBP2 likely also contributed to increased hepatic glyceride accumulation, since overexpression of SREBP2 similarly induces transcription of lipogenic (*Acc1*, *Acc2*, *Fas*) genes (106; 116). Finally, concomitant reduced expression of phosphatidylcholine transport protein (PCTP) may have also contributed toward hepatic phospholipid retention, as this protein is considered to mediate intracellular phospholipid transfer. It is important to note that the DKO did not significantly upregulate other key proteins in LCFA uptake (FATP2, FATP4), transport (ACBP), oxidation (ACBP, CPT1), or alter serum levels of β -hydroxybutyrate—an *in vivo* measure of LCFA β -oxidation.

DKO Exacerbated the Induced Hepatic Glyceride Accumulation Observed in Mice Fed a High Cholesterol Diet

The DKO exacerbated cholesterol diet-induced hepatic accumulation of glycerides (phospholipid and triacylglyceride). This exacerbation, occurring primarily in females but not males, was associated with decreased expression of: i) *Ceh/Hsl* which would favor cholesteryl ester accumulation; ii) MTP (due to increased SREBP1 and SREBP2, both of which inhibit MTP transcription) which loads ApoB with triglyceride and cholesteryl ester, and iii) ApoB which would decreased the level of ApoB available for loading with glycerides and cholesteryl ester. Together these factors would elicit

glyceride and cholesteryl accumulation as a result of decreased hepatic secretion of nascent VLDL and LDL.

DKO Mouse Construct and Study Design Differences in Comparison to a Previous Study

The phenotype of control-fed DKO mice in this study differed significantly from that reported in an earlier study with independently-created male DKO mice (104). In the latter study, body weights were unaltered despite increased food intake, hepatic accumulation of cholesterol (especially cholesteryl ester) as well as glycerides (phospholipid and/or triglyceride) was not observed, and hepatic levels of phospholipid were unaltered, while triglycerides decreased (104). The earlier study differed in several key aspects since the DKO mice used therein were: i) generated using a different ablation construct strategy (104); ii) backcrossed to a different background substrain (C57BL/6J rather than C57BL/6N). The C57BL/6J mice differ significantly from C57BL/6N mice in a number of genes and are normally much more susceptible to high fat diet-induced obesity (rev. in (4)); iii) The C57BL/6J mice were fed a control diet containing 0.2 mg phytanic acid/g food as well as 0.08 mg phytol/g food (104).

In contrast, the diet in the present study was prepared phytoestrogen-free and phytanic acid/phytol free, as confirmed by gas chromatography/mass spectroscopic analysis which indicated no detectable phytanic acid. Phytol was present only at 0.0028 ± 0.0004 mg/g food. Phytanic acid is a ligand for both L-FABP and PPAR α (22; 38; 63) and is one of the most potent naturally-occurring inducers of PPAR α (1; 33; 122). L-FABP is known to transport bound fatty acids into nuclei wherein it directly

interacts with (37; 40; 107; 117; 120) and facilitate ligand activation of PPAR α (37; 40; 44; 80; 81; 120). Ligand induction of PPAR α elicits transcription of L-FABP as well as multiple enzymes involved in LCFA oxidation (44; 80; 81; 102; 120).

Thus, the seventy-one fold higher dietary level of phytanic acid in the control chow of the previous study in C576BL/6J mice would be expected to significantly induce PPAR α transcription of L-FABP as confirmed by fivefold concomitant upregulation of L-FABP (25; 104); nearly three to fivefold greater than the present study. The much higher induction of L-FABP in turn would reinforce or potentiate phytanic acid uptake and transport into the nucleus to induce PPAR α transcription of LCFA oxidative enzymes and reduce hepatic levels of fatty acids acylated to phospholipid and triglyceride (104). Since phytanic acid and pristanic acid are very potent PPAR α agonists that induce transcription of fatty acid oxidative enzymes and L-FABP, increased fatty acid oxidation would compensate for any increase in food consumption and thereby maintain body weight (7; 9; 18; 34). Thus the significant dietary content of branched-chain lipids (phytanic acid, phytol) in the earlier study would account for the differences in the presently observed phenotype.

CONCLUSION

In conclusion, the SCP-2/SCP-x double gene ablation (DKO) elicited hepatic lipid accumulation, especially of cholesteryl esters and glycerides (phospholipid and/or triglyceride). This lipid accumulation was associated primarily with: i) loss of SCP-2; ii) concomitant upregulation of L-FABP; and/or iii) increased protein levels of the nuclear receptors SREBP1 and SREBP2. Upregulation of L-FABP in control-fed male DKO mice is important to both fatty acid and cholesterol metabolism, since L-FABP binds and enhances the uptake, transport, and esterification of both fatty acid and cholesterol. Further, the DKO increased hepatic protein levels of both SREBP1 and SREBP2 in control-fed males and females as well as in cholesterol-fed female DKO mice. These proteins regulate transcription of lipogenic (SREBP1, SREBP2) and cholesterologenic (SREBP2) genes. Finally, DKO exacerbated the cholesterol diet-induced hepatic accumulation of cholesteryl esters and glycerides. However, this exacerbation was associated with multiple factors, including loss of SCP-2 and decreased expression of *Ceh/Hsl*, MTP, and Apo B. Taken together, these findings were consistent with the hypothesized role for SCP-2 in targeting cholesterol transport to the ER to stimulate ACAT2-mediated cholesteryl ester formation (14; 15; 29; 45; 74; 79). In addition, the data suggested a potential novel role for SCP-2 in cholesterol transfer to ER to regulate release of SREBP1 and 2, key nuclear receptors in lipogenesis and cholesterologenesis.

REFERENCES

1. Adida A and Spener F. Intracellular lipid binding proteins and nuclear receptors involved in branched-chain fatty acid signaling. *Prost Leukot Essen Fatty Acids* 67: 91-98, 2002.
2. Amigo L, Zanlungo S, Miquel JF, Glick JM, Hyogo H, Cohen DE, Rigotti A and Nervi F. Hepatic overexpression of sterol carrier protein-2 inhibits VLDL production and reciprocally enhances biliary lipid secretion. *J Lipid Res* 44: 399-407, 2003.
3. Atshaves BP, Gallegos A, McIntosh AL, Kier AB and Schroeder F. Sterol carrier protein-2 selectively alters lipid composition and cholesterol dynamics of caveolae/lipid raft vs non-raft domains in L-cell fibroblast plasma membranes. *Biochemistry* 42: 14583-14598, 2003.
4. Atshaves BP, Martin GG, Hostetler HA, McIntosh AL, Kier AB and Schroeder F. Liver fatty acid binding protein (L-FABP) and dietary obesity. *Journal of Nutritional Biochemistry* 21: 1015-1032, 2010.
5. Atshaves BP, McIntosh AL, Martin GG, Landrock D, Payne HR, Bhuvanendran S, Landrock K, Lyuksyutova OI, Johnson JD, Macfarlane RD, Kier AB and Schroeder F. Overexpression of sterol carrier protein-2 differentially alters hepatic cholesterol accumulation in cholesterol-fed mice. *J Lipid Res* 50: 1429-1447, 2009.
6. Atshaves BP, McIntosh AL, Landrock D, Payne HR, Mackie J, Maeda N, Ball JM, Schroeder F and Kier AB. Effect of SCP-x gene ablation on branched-chain fatty acid metabolism. *Am J Physiol* 292: 939-951, 2007.

7. Atshaves BP, McIntosh AL, Lyuksyutova OI, Zipfel WR, Webb WW and Schroeder F. Liver fatty acid binding protein gene ablation inhibits branched-chain fatty acid metabolism in cultured primary hepatocytes. *J Biol Chem* 279: 30954-30965, 2004.
8. Atshaves BP, McIntosh AL, Payne HR, Gallegos AM, Landrock K, Maeda N, Kier AB and Schroeder F. Sterol carrier protein-2/sterol carrier protein-x gene ablation alters lipid raft domains in primary cultured mouse hepatocytes. *J Lipid Res* 48: 2193-2211, 2007.
9. Atshaves BP, Payne HR, McIntosh AL, Tichy SE, Russell D, Kier AB and Schroeder F. Sexually dimorphic metabolism of branched chain lipids in C57BL/6J mice. *J Lipid Res* 45: 812-830, 2004.
10. Atshaves BP, Petrescu A, Starodub O, Roths J, Kier AB and Schroeder F. Expression and intracellular processing of the 58 kDa sterol carrier protein 2/3-oxoacyl-CoA thiolase in transfected mouse L-cell fibroblasts. *J Lipid Res* 40: 610-622, 1999.
11. Atshaves BP, Starodub O, McIntosh AL, Roths JB, Kier AB and Schroeder F. Sterol carrier protein-2 alters HDL-mediated cholesterol efflux. *J Biol Chem* 275: 36852-36861, 2000.
12. Atshaves BP, Storey S, Huang H and Schroeder F. Liver fatty acid binding protein expression enhances branched-chain fatty acid metabolism. *Mol Cell Biochem* 259: 115-129, 2004.
13. Bordewick U, Heese M, Borchers T, Robenek H and Spener F. Compartmentation of hepatic fatty-acid-binding protein in liver cells and its effect on microsomal phosphatidic acid biosynthesis. *Biol Chem Hoppe-Seyler* 370: 229-238, 1989.

14. Chao H, Martin G, Russell WK, Waghela SD, Russell DH, Schroeder F and Kier AB. Membrane charge and curvature determine interaction with acyl CoA binding protein (ACBP) and fatty acyl CoA targeting. *Biochemistry* 41: 10540-10553, 2002.
15. Chao H, Zhou M, McIntosh A, Schroeder F and Kier AB. Acyl CoA binding protein and cholesterol differentially alter fatty acyl CoA utilization by microsomal acyl CoA: cholesterol transferase. *J Lipid Res* 44: 72-83, 2003.
16. Cohen DE. Hepatocellular transport and secretion of biliary lipids. *Cur Opin Lipidology* 10: 295-302, 1999.
17. Colles SM, Woodford JK, Moncecchi D, Myers-Payne SC, McLean LR, Billheimer JT and Schroeder F. Cholesterol interactions with recombinant human sterol carrier protein-2. *Lipids* 30: 795-804, 1995.
18. Ellinghaus P, Wolfrum C, Assmann G, Spener F and Seedorf U. Phytanic acid activates the peroxisome proliferator-activated receptor alpha (PPARalpha) in sterol carrier protein-2-/sterol carrier protein x-deficient mice. *J Biol Chem* 274: 2766-2772, 1999.
19. Ferdinandusse S, Kostopoulos P, Denis S, Rusch R, Overmars H, Dillman U, Reith W, Haas D, Wanders RJA, Duran M and Marziniak M. Mutations in the gene encoding peroxisomal sterol carrier protein-x (SCP-x) cause leukencephalopathy with dystonia and motor neuropathy. *Am J Hum Genet* 78: 1046-1052, 2006.
20. Frikke-Schmidt R. Genetic variation in the ABCA1 gene, HDL cholesterol, and risk of ischemic heart disease in the general population. *Atherosclerosis* 208: 305-316, 2010.
21. Frolov A, Cho TH, Billheimer JT and Schroeder F. Sterol carrier protein-2, a new fatty acyl coenzyme A-binding protein. *J Biol Chem* 271: 31878-31884, 1996.

22. Frolov A, Miller K, Billheimer JT, Cho T-C and Schroeder F. Lipid specificity and location of the sterol carrier protein-2 fatty acid binding site: A fluorescence displacement and energy transfer study. *Lipids* 32: 1201-1209, 1997.
23. Frolov A, Woodford JK, Murphy EJ, Billheimer JT and Schroeder F. Spontaneous and protein-mediated sterol transfer between intracellular membranes. *J Biol Chem* 271: 16075-16083, 1996.
24. Frolov AA, Woodford JK, Murphy EJ, Billheimer JT and Schroeder F. Fibroblast membrane sterol kinetic domains: modulation by sterol carrier protein 2 and liver fatty acid binding protein. *J Lipid Res* 37: 1862-1874, 1996.
25. Fuchs M, Hafer A, Muench C, Kannenberg F, Teichmann S, Scheibner J, Stange EF and Seedorf U. Disruption of the sterol carrier protein 2 gene in mice impairs biliary lipid and hepatic cholesterol metabolism. *J Biol Chem* 276: 48058-48065, 2001.
26. Gallegos AM, Atshaves BP, McIntosh AL, Storey SM, Ball JM, Kier AB and Schroeder F. Membrane domain distributions: Analysis of fluorescent sterol exchange kinetics. *Current Analytical Chemistry* 4: 1-7, 2008.
27. Gallegos AM, Atshaves BP, Storey S, McIntosh A, Petrescu AD and Schroeder F. Sterol carrier protein-2 expression alters plasma membrane lipid distribution and cholesterol dynamics. *Biochemistry* 40: 6493-6506, 2001.
28. Gallegos AM, Atshaves BP, Storey SM, Schoer J, Kier AB and Schroeder F. Molecular and fluorescent sterol approaches to probing lysosomal membrane lipid dynamics. *Chem Phys Lipids* 116: 19-38, 2002.

29. Gallegos AM, Atshaves BP, Storey SM, Starodub O, Petrescu AD, Huang H, McIntosh A, Martin G, Chao H, Kier AB and Schroeder F. Gene structure, intracellular localization, and functional roles of sterol carrier protein-2. *Prog Lipid Res* 40: 498-563, 2001.
30. Gallegos AM, McIntosh AL, Atshaves BP and Schroeder F. Structure and cholesterol domain dynamics of an enriched caveolae/raft isolate. *Biochem J* 382: 451-461, 2004.
31. Gallegos AM, Storey SM, Kier AB, Schroeder F and Ball JM. Structure and cholesterol dynamics of caveolae/raft and nonraft plasma membrane domains. *Biochemistry* 45: 12100-12116, 2006.
32. Gavey KL, Noland BJ and Scallen TJ. The participation of sterol carrier protein2 in the conversion of cholesterol to cholesterol ester by rat liver microsomes. *J Biol Chem* 256: 2993-2999, 1981.
33. Hanhoff T, Benjamin S, Borchers T and Spener F. Branched-chain fatty acids as activators of peroxisome proliferators. *Eur J Lip Sci Technol* 107: 716-729, 2005.
34. Hanhoff T, Wolfrum C, Ellinghaus P, Seedorf U and Spener F. Pristanic acid is activator of PPARalpha. *Eur J Lipid Sci* 103: 75-80, 2001.
35. Hazard SE and Patel SB. Sterolins ABCG5 and ABCG8: regulators of whole body dietary sterols. *Pflugers Arch* 453: 745-752, 2007.
36. Horton J.D., Goldstein J.L. and Brown M.S. SREBPs: activators of the complete program of cholesterol and fatty acid synthesis in the liver. *J Clin Invest* 109: 1125-1131, 2002.

37. Hostetler HA, Balanarasimha M, Huang H, Kelzer MS, Kaliappan A, Kier AB and Schroeder F. Glucose regulates fatty acid binding protein interaction with lipids and PPAR α . *J Lipid Res* 51: 3103-3116, 2010.
38. Hostetler HA, Kier AB and Schroeder F. Very-long-chain and branched-chain fatty acyl CoAs are high affinity ligands for the peroxisome proliferator-activated receptor alpha (PPAR α). *Biochemistry* 45: 7669-7681, 2006.
39. Hostetler HA, Lupas D, Tan Y, Dai J, Kelzer MS, Martin GG, Woldegiorgis G, Kier AB and Schroeder F. Acyl-CoA binding proteins interact with the acyl-CoA binding domain of mitochondrial carnitine palmitoyltransferase I. *Mol Cell Biochem* 355: 135-148, 2011.
40. Hostetler HA, McIntosh AL, Atshaves BP, Storey SM, Payne HR, Kier AB and Schroeder F. Liver type fatty acid binding protein (L-FABP) interacts with peroxisome proliferator activated receptor- α in cultured primary hepatocytes. *J Lipid Res* 50: 1663-1675, 2009.
41. Huang H, Gallegos A, Zhou M, Ball JM and Schroeder F. Role of sterol carrier protein-2 N-terminal membrane binding domain in sterol transfer. *Biochemistry* 41: 12149-12162, 2002.
42. Huang H, McIntosh AL, Martin GG, Landrock K, Landrock D, Gupta S, Atshaves BP, Kier AB and Schroeder F. Structural and functional interaction of fatty acids with human liver fatty acid binding protein (L-FABP) T94A variant. *FEBS J* 281: 2266-2283, 2014.
43. Huang H, McIntosh AL, Martin GG, Landrock KK, Landrock D, Storey SM, Gupta S, Atshaves BP, Kier AB and Schroeder F. Human L-FABP T94A variant enhances cholesterol uptake. *Biochim Biophys Acta* Revision Pending 10/5/14: 2014.

44. Huang H, McIntosh AL, Martin GG, Petrescu AD, Landrock K, Landrock D, Kier AB and Schroeder F. Inhibitors of fatty acid synthesis induce PPAR α -regulated fatty acid β -oxidative enzymes: synergistic roles of L-FABP and glucose. *PPAR Research* 2013: 1-22, 2013.
45. Jefferson JR, Slotte JP, Nemezc G, Pastuszyn A, Scallen TJ and Schroeder F. Intracellular sterol distribution in transfected mouse L-cell fibroblasts expressing rat liver fatty acid binding protein. *J Biol Chem* 266: 5486-5496, 1991.
46. Jolly CA, Chao H, Kier AB, Billheimer JT and Schroeder F. Sterol carrier protein-2 suppresses microsomal acyl CoA hydrolysis. *Mol Cell Biochem* 205: 83-90, 2000.
47. Jolly CA, Hubbell T, Behnke WD and Schroeder F. Fatty acid binding protein: Stimulation of microsomal phosphatidic acid formation. *Arch Biochem Biophys* 341: 112-121, 1997.
48. Jolly CA, Murphy EJ and Schroeder F. Differential influence of rat liver fatty acid binding protein isoforms on phospholipid fatty acid composition: phosphatidic acid biosynthesis and phospholipid fatty acid remodeling. *Biochim Biophys Acta* 1390: 258-268, 1998.
49. Jolly CA, Wilton DA and Schroeder F. Microsomal fatty acyl CoA transacylation and hydrolysis: fatty acyl CoA species dependent modulation by liver fatty acyl CoA binding proteins. *Biochim Biophys Acta* 1483: 185-197, 2000.
50. Kannenberg F, Ellinghaus P, Assmann G and Seedorf U. Aberrant oxidation of the cholesterol side chain in bile acid synthesis of sterol carrier protein-2/sterol carrier protein-x knockout mice. *J Biol Chem* 274: 35455-35460, 1999.

51. Kawata S, Imai Y, Inada M, Inui M, Kakimoto H, Fukuda K, Maeda Y and Tarui S. Modulation of cholesterol 7- α hydroxylase activity by nsLTP in human liver - possible altered regulation of its cytosolic level in patients with gallstones. *Clin Chim Acta* 197: 201-208, 1991.
52. Kim HJ, Miyazaki M and Ntambi JM. Dietary cholesterol opposes PUFA-mediated repression of stearoyl-CoA desaturase-1 gene by SREBP-1 independent mechanism. *J Lipid Res* 43: 1750-1757, 2002.
53. Li F, Patterson AD, Krausz KW, Tanaka N and Gonzalez FJ. Metabolomics reveals an essential role for PPAR α in bile acid homeostasis. *J Lipid Res* 53: 1625-1635, 2012.
54. Li T and Chiang JYL. Regulation of bile acid and cholesterol metabolism by PPARs. *PPAR Research* 2009: Article ID 501739-15, 2009.
55. Maatman RG, van Moerkerk HT, Nooren IM, van Zoelen EJ and Veerkamp JH. Expression of human liver fatty acid-binding protein in Escherichia coli and comparative analysis of its binding characteristics with muscle fatty acid-binding protein. *Biochim Biophys Acta* 1214: 1-10, 1994.
56. Mackie JT, Atshaves BP, Payne HR, McIntosh AL, Schroeder F and Kier AB. Phytol-induced hepatotoxicity in mice. *Toxicol Pathol* 37: 201-208, 2009.
57. Martin GG, Atshaves BP, Landrock KK, Landrock D, Storey SM, Howles PN, Kier AB and Schroeder F. Ablating L-FABP in SCP-2/SCP-x null mice impairs bile acid metabolism and biliary HDL-cholesterol secretion. *Am J Physiol Gastrointest and Liver Phys* Accepted 10-2-14: 10.1152/ajpgi.00209.2014, 2014.

58. Martin GG, Atshaves BP, McIntosh AL, Mackie JT, Kier AB and Schroeder F. Liver fatty acid binding protein (L-FABP) gene ablation alters liver bile acid metabolism in male mice. *Biochem J* 391: 549-560, 2005.
59. Martin GG, Atshaves BP, McIntosh AL, Mackie JT, Kier AB and Schroeder F. Liver fatty acid binding protein (L-FABP) gene ablation potentiates hepatic cholesterol accumulation in cholesterol-fed female mice. *Am J Physiol* 290: G36-G48, 2006.
60. Martin GG, Danneberg H, Kumar LS, Atshaves BP, Erol E, Bader M, Schroeder F and Binas B. Decreased liver fatty acid binding capacity and altered liver lipid distribution in mice lacking the liver fatty acid binding protein (L-FABP) gene. *J Biol Chem* 278: 21429-21438, 2003.
61. Martin GG, Hostetler HA, McIntosh AL, Tichy SE, Williams BJ, Russell DH, Berg JM, Spencer TA, Ball JA, Kier AB and Schroeder F. Structure and function of the sterol carrier protein-2 (SCP-2) N-terminal pre-sequence. *Biochem* 47: 5915-5934, 2008.
62. Martin GG, Huang H, Atshaves BP, Binas B and Schroeder F. Ablation of the liver fatty acid binding protein gene decreases fatty acyl CoA binding capacity and alters fatty acyl CoA pool distribution in mouse liver. *Biochem* 42: 11520-11532, 2003.
63. Martin GG, McIntosh AL, Huang H, Gupta S, Atshaves BP, Kier AB and Schroeder F. Human liver fatty acid binding protein (L-FABP) T94A variant alters structure, stability, and interaction with fibrates. *Biochemistry* 52: 9347-9357, 2013.
64. McIntosh AL, Atshaves BP, Huang H, Gallegos AM, Kier AB and Schroeder F. Fluorescence techniques using dehydroergosterol to study cholesterol trafficking. *Lipids* 43: 1185-1208, 2008.

65. McIntosh AL, Huang H, Atshaves BP, Storey SM, Gallegos A, Spencer TA, Bittman R, Ohno-Iwashita Y, Kier AB and Schroeder F. Fluorescent sterols for the study of cholesterol trafficking in living cells. In: *Probes and Tags to Study Biomolecular Function for Proteins, RNA, and Membranes.*, edited by Miller LW. Weinheim: Wiley VCH Verlag GmbH & Co., 2008, p. 1-33.
66. McIntosh AL, Huang H, Atshaves BP, Wellburg E, Kuklev DV, Smith WL, Kier AB and Schroeder F. Fluorescent n-3 and n-6 very long chain polyunsaturated fatty acids: three photon imaging and metabolism in living cells overexpressing liver fatty acid binding protein. *J Biol Chem* 285: 18693-18708, 2010.
67. McIntosh AL, Huang H, Storey SM, Landrock K, Landrock D., Petrescu AD, Gupta S, Atshaves BP, Kier AB and Schroeder F. Human FABP1 T94A variant impacts fatty acid metabolism and PPAR α activation in cultured human female hepatocytes. *Am J Physiol Gastrointest and Liver Phys* 307: G164-G176, 2014.
68. Moncecchi DM, Murphy EJ, Prows DR and Schroeder F. Sterol carrier protein-2 expression in mouse L-cell fibroblasts alters cholesterol uptake. *Biochim Biophys Acta* 1302: 110-116, 1996.
69. Moncecchi DM, Nemezc G, Schroeder F and Scallen TJ. The participation of sterol carrier protein-2 (SCP-2) in cholesterol metabolism. In: *Physiology and Biochemistry of Sterols*, edited by Patterson GW and Nes WD. Champaign, IL: American Oil Chemists' Society Press, 1991, p. 1-27.
70. Murphy EJ. L-FABP and I-FABP expression increase NBD-stearate uptake and cytoplasmic diffusion in L-cells. *Am J Physiol* 275: G244-G249, 1998.

71. Murphy EJ. Sterol carrier protein-2 expression increases fatty acid uptake and cytoplasmic diffusion in L-cell fibroblasts. *Am J Physiol* 275: G237-G243, 1998.
72. Murphy EJ, Prows DR, Jefferson JR, Incerpi S, Hertelendy ZI, Heiliger CE and Schroeder F. Cis-parinaric acid uptake in L-cells. *Arch Biochem Biophys* 335: 267-272, 1996.
73. Murphy EJ, Prows DR, Jefferson JR and Schroeder F. Liver fatty acid binding protein expression in transfected fibroblasts stimulates fatty acid uptake and metabolism. *Biochim Biophys Acta* 1301: 191-198, 1996.
74. Murphy EJ and Schroeder F. Sterol carrier protein-2 mediated cholesterol esterification in transfected L-cell fibroblasts. *Biochim Biophys Acta* 1345: 283-292, 1997.
75. Musso G, Bo S, Cassader M, De Michieli F and Gambino R. Impact of sterol regulatory element-binding factor-1c polymorphism on incidence of NAFLD and on the severity of liver disease and of glucose and lipid dysmetabolism. *Am J Clin Nutr* 98: 895-906, 2013.
76. Myers-Payne SC, Hubbell T, Wood WG and Schroeder F. Effects of *in vitro* and *in vivo* ethanol on liver cytosolic lipid binding proteins. *Hepatology* 1995.
77. Nagy TR and Clair A-L. Precision and accuracy of dual-energy X-ray absorptiometry for *in vivo* body composition in mice. *Obesity Research* 8: 392-398, 2000.
78. Navab M, Anantharamaiah GM, Reddy ST, Van Lenten BJ and Fogelman AM. HDL as a biomarker, potential therapeutic target, and therapy. *Diabetes* 58: 2711-2717, 2009.
79. Nemezc G and Schroeder F. Selective binding of cholesterol by recombinant fatty acid-binding proteins. *J Biol Chem* 266: 17180-17186, 1991.

80. Petrescu AD, Huang H, Martin GG, McIntosh AL, Storey SM, Landrock D, Kier AB and Schroeder F. Impact of L-FABP and glucose on polyunsaturated fatty acid induction of PPAR α regulated β -oxidative enzymes. *Am J Physiol Gastrointest and Liver Phys* 304: G241-G256, 2013.
81. Petrescu AD, McIntosh AL, Storey SM, Huang H, Martin GG, Landrock D, Kier AB and Schroeder F. High glucose potentiates liver fatty acid binding protein (L-FABP) mediated fibrate induction of PPAR α in mouse hepatocytes. *Biochim Biophys Acta* 1831: 1412-1425, 2013.
82. Prows DR, Murphy EJ and Schroeder F. Intestinal and liver fatty acid binding proteins differentially affect fatty acid uptake and esterification in L-Cells. *Lipids* 30: 907-910, 1995.
83. Puglielli L, Rigotti A, Amigo L, Nunez L, Greco AV, Santos MJ and Nervi F. Modulation on intrahepatic cholesterol trafficking: Evidence by *in vivo* antisense treatment for the involvement of sterol carrier protein-2 in newly synthesized cholesterol transfer into bile. *Biochem J* 317: 681-687, 1996.
84. Repa JJ and Mangelsdorf DJ. The role of orphan nuclear receptors in the regulation of cholesterol homeostasis. *Annu Rev Cell Dev Biol* 16: 459-481, 2000.
85. Richieri GV, Ogata RT and Kleinfeld AM. Equilibrium constants for the binding of fatty acids with fatty acid binding proteins from adipocyte, intestine, heart, and liver measured with the fluorescent probe ADIFAB. *J Biol Chem* 269: 23918-23930, 1994.
86. Robins SJ and Fasulo JM. High density lipoproteins, but not other lipoproteins, provide a vehicle for sterol transport to the bile. *J Clin Inv* 99: 380-384, 1997.

87. Robins SJ and Fasulo JM. Delineation of a novel hepatic route for the selective transfer of unesterified sterols from high density lipoproteins to bile: studies using the perfused rat liver. *Hepatology* 29: 1541-1548, 1999.
88. Rubin D, Schneider-Muntau A, Klapper M, Nitz I, Helwig U, Folsch UR, Schrezenmeir J and Doring F. Functional analysis of promoter variants in the MTTP gene. *Human Mutation* 29: 123-129, 2008.
89. Russell DW. The enzymes, regulation, and genetics of bile acid synthesis. *Annu Rev Biochem* 72: 137-174, 2003.
90. Sato R, Miyamoto W, Inoue J, Terada T, Imanaka T and Maeda M. SREBP negatively regulates MTTP gene transcription. *J Biol Chem* 274: 24714-24720, 1999.
91. Schaefer EJ, Santos RD and Asztalos BF. Marked HDL deficiency and premature coronary heart disease. *Curr Opin Lipidol* 21: 289-297, 2010.
92. Schoer J, Gallegos A, Starodub O, Petrescu A, Roths JB, Kier AB and Schroeder F. Lysosomal membrane cholesterol dynamics: role of sterol carrier protein-2 gene products. *Biochemistry* 39: 7662-7677, 2000.
93. Schroeder F, Butko P, Nemezc G and Scallen TJ. Interaction of fluorescent delta 5,7,9(11),22-ergostetraen-3b-ol with sterol carrier protein-2. *J Biol Chem* 265: 151-157, 1990.
94. Schroeder F, Frolov A, Schoer J, Gallegos A, Atshaves BP, Stolowich NJ, Scott AI and Kier AB. Intracellular sterol binding proteins, cholesterol transport and membrane domains. In: *Intracellular cholesterol trafficking*, edited by Chang TY and Freeman DA. Boston: Kluwer Academic Publishers, 1998, p. 213-234.

95. Schroeder F, Frolov A, Starodub O, Russell W, Atshaves BP, Petrescu AD, Huang H, Gallegos A, McIntosh A, Tahotna D, Russell D, Billheimer JT, Baum CL and Kier AB. Pro-sterol carrier protein-2: role of the N-terminal presequence in structure, function, and peroxisomal targeting. *J Biol Chem* 275: 25547-25555, 2000.
96. Schroeder F, Frolov AA, Murphy EJ, Atshaves BP, Jefferson JR, Pu L, Wood WG, Foxworth WB and Kier AB. Recent advances in membrane cholesterol domain dynamics and intracellular cholesterol trafficking. *Proc Soc Exp Biol Med* 213: 150-177, 1996.
97. Schroeder F, Gallegos AM, Atshaves BP, Storey SM, McIntosh A, Petrescu AD, Huang H, Starodub O, Chao H, Yang H, Frolov A and Kier AB. Recent advances in membrane cholesterol microdomains: rafts, caveolae, and intracellular cholesterol trafficking. *Experimental Biology and Medicine* 226: 873-890, 2001.
98. Schroeder F, Huang H, McIntosh AL, Atshaves BP, Martin GG and Kier AB. Caveolin, sterol carrier protein-2, membrane cholesterol-rich microdomains and intracellular cholesterol trafficking. In: *Cholesterol binding and cholesterol transport proteins*, edited by Harris JR. New York: Springer SBM, 2010, p. 279-318.
99. Schroeder F, Jefferson JR, Kier AB, Knittell J, Scallen TJ, Wood WG and Hapala I. Membrane cholesterol dynamics: cholesterol domains and kinetic pools. *Proc Soc Exp Biol Med* 196: 235-252, 1991.
100. Schroeder F, Jolly CA, Cho TH and Frolov AA. Fatty acid binding protein isoforms: structure and function. *Chem Phys Lipids* 92: 1-25, 1998.

101. Schroeder F, Myers-Payne SC, Billheimer JT and Wood WG. Probing the ligand binding sites of fatty acid and sterol carrier proteins: effects of ethanol. *Biochemistry* 34: 11919-11927, 1995.
102. Schroeder F, Petrescu AD, Huang H, Atshaves BP, McIntosh AL, Martin GG, Hostetler HA, Vespa A, Landrock K, Landrock D, Payne HR and Kier AB. Role of fatty acid binding proteins and long chain fatty acids in modulating nuclear receptors and gene transcription. *Lipids* 43: 1-17, 2008.
103. Seedorf U, Brysch P, Engel T, Schrage K and Assmann G. Sterol carrier protein X is peroxisomal 3-oxoacyl coenzyme A thiolase with intrinsic sterol carrier and lipid transfer activity. *J Biol Chem* 269: 21277-21283, 1994.
104. Seedorf U, Raabe M, Ellinghaus P, Kannenberg F, Fobker M, Engel T, Denis S, Wouters F, Wirtz KWA, Wanders RJA, Maeda N and Assmann G. Defective peroxisomal catabolism of branched fatty acyl coenzyme A in mice lacking the sterol carrier protein-2/sterol carrier protein-x gene function. *Genes and Development* 12: 1189-1201, 1998.
105. Seltman H, Diven W, Rizk M, Noland BJ, Chanderbhan R and Scallen TJ. Regulation of bile-acid synthesis. Role of sterol carrier protein 2 in biosynthesis of 7 alpha-hydroxy-cholesterol. *Biochem J* 230: 879-884, 1985.
106. Shimano H. SREBPs: transcriptional regulators of lipid synthetic genes. *Prog Lipid Res* 40: 439-452, 2001.

107. Smathers RL, Galligan JJ, Shearn CT, Fritz KS, Mercer K, Ronis M, Orlicky DJ, Davidson NO and Petersen DR. Susceptibility of L-FABP $-/-$ mice to oxidative stress in early-stage alcoholic liver. *J Lipid Res* 54: 1335-1345, 2013.
108. Starodub O, Jolly CA, Atshaves BP, Roths JB, Murphy EJ, Kier AB and Schroeder F. Sterol carrier protein-2 immunolocalization in endoplasmic reticulum and stimulation of phospholipid formation. *Am J Physiol* 279: C1259-C1269, 2000.
109. Stolowich NJ, Frolov A, Petrescu AD, Scott AI, Billheimer JT and Schroeder F. Holo-sterol carrier protein-2: ^{13}C -NMR investigation of cholesterol and fatty acid binding sites. *J Biol Chem* 274: 35425-35433, 1999.
110. Storey SM, Atshaves BP, McIntosh AL, Landrock KK, Martin GG, Huang H, Johnson JD, Macfarlane RD, Kier AB and Schroeder F. Effect of sterol carrier protein-2 gene ablation on HDL-mediated cholesterol efflux from primary cultured mouse hepatocytes. *Am J Physiol* 299: 244-254, 2010.
111. Storey SM, Gallegos AM, Atshaves BP, McIntosh AL, Martin GG, Landrock K, Kier AB, Ball JA and Schroeder F. Selective cholesterol dynamics between lipoproteins and caveolae/lipid rafts. *Biochemistry* 46: 13891-13906, 2007.
112. Storey SM, McIntosh AL, Huang H, Martin GG, Landrock KK, Landrock D., Payne HR, Kier AB and Schroeder F. Intracellular cholesterol binding proteins enhance HDL-mediated cholesterol uptake in cultured primary mouse hepatocytes. *Am J Physiol Gastrointest and Liver Phys* 302: G824-G839, 2012.

113. Thigpen JE, Setchell KD, Ahlmark KB, Kocklear J, Spahr T, Caviness GF, Goelz MF, Haseman JK, Newbold RR and Forsythe DB. Phytoestrogen content of purified, open- and closed-formula laboratory animal diets. *Lab An Science* 49: 530-536, 1999.
114. Thigpen JE, Setchell KD, Goelz MF and Forsythe DB. The phytoestrogen content of rodent diets. *Environ Health Persp* 107: A182-A183, 1999.
115. Trauner M and Boyer JL. Bile salt transporters: Molecular characterization, function, and regulation. *Physiol Rev* 83: 633-671, 2003.
116. Vallim T and Salter AM. Regulation of hepatic gene expression by saturated fatty acids. *Prost Leukot Essen Fatty Acids* 82: 211-218, 2010.
117. Velkov T. Interactions between human liver fatty acid binding protein and peroxisome proliferator activated receptor drugs. *PPAR Research* 2013: 1-14, 2013.
118. Weisiger RA. Cytosolic fatty acid binding proteins catalyze two distinct steps in intracellular transport of their ligands. *Mol Cell Biochem* 239: 35-42, 2005.
119. Wolfrum C, Borchers T, Sacchettini JC and Spener F. Binding of fatty acids and peroxisome proliferators to orthologous fatty acid binding proteins from human, murine, and bovine liver. *Biochemistry* 39: 1469-1474, 2000.
120. Wolfrum C, Borrmann CM, Borchers T and Spener F. Fatty acids and hypolipidemic drugs regulate PPARalpha and PPARgamma gene expression via L-FABP: a signaling path to the nucleus. *Proc Natl Acad Sci* 98: 2323-2328, 2001.
121. Wolfrum C, Buhlman C, Rolf B, Borchers T and Spener F. Variation of liver fatty acid binding protein content in the human hepatoma cell line HepG2 by peroxisome

- proliferators and antisense RNA affects the rate of fatty acid uptake. *Biochim Biophys Acta* 1437: 194-201, 1999.
122. Wolfrum C, Ellinghaus P, Fobker M, Seedorf U, Assmann G, Borchers T and Spener F. Phytanic acid is ligand and transcriptional activator of murine liver fatty acid binding protein. *J Lipid Res* 40: 708-714, 1999.
123. Woodford JK, Colles SM, Myers-Payne S, Billheimer JT and Schroeder F. Sterol carrier protein-2 stimulates intermembrane sterol transfer by direct membrane interaction. *Chem Phys Lipids* 76: 73-84, 1995.
124. Woodford JK, Hapala I, Jefferson JR, Knittel JJ, Kavecansky J, Powell D, Scallen TJ and Schroeder F. Mechanistic studies of sterol carrier protein-2 effects on L- cell fibroblast plasma membrane sterol domains. *Biochim Biophys Acta* 1189: 52-60, 1994.
125. Zanolungo S, Amigo L, Mendoza H, Glick J, Rodriguez A, Kozarsky K, Miquel JF, Rigotti A and Nervi F. Overexpression of sterol carrier protein-2 in mice leads to increased hepatic cholesterol content and enterohepatic circulation of bile acids. *Gastroenterology* 118: 135 A1165., 2000.
126. Zanolungo S, Rigotti A and Nervi F. Hepatic cholesterol transport from plasma into bile: implications for gallstone disease. *Cur Opin Lipidology* 15: 279-286, 2004.
127. Zhou M, Parr RD, Petrescu AD, Payne HR, Atshaves BP, Kier AB, Ball JA and Schroeder F. Sterol carrier protein-2 directly interacts with caveolin-1 *in vitro* and *in vivo*. *Biochemistry* 43: 7288-7306, 2004